Research Experience

List of Publication:

- **Ruchika**, Kumari S., Dhiman P., Singh D., Saneja A.* (2022). *R*-*α*-Lipoic Acid Conjugated to *D*-*α*-Tocopherol Polyethylene Glycol 1000 Succinate: Synthesis, Characterization, and Effect on Antiseizure Activity. **Journal of Agricultural and Food Chemistry,** 70, 25, 7674–7682 https://doi.org/10.1021/acs.jafc.2c01685 **(IF:5.895)**

- **Ruchika**, Sharma A., Saneja A.* (2022). Zebrafish as A Powerful Alternative Model Organism for Preclinical Investigation of Nanomedicines, **Drug Discovery Today**, 27, 5, 1513 - 1522 https://doi.org/10.1016/j.drudis.2022.02.011 **(IF: 8.369)**

- Dhritlahre R. K., **Ruchika**, Padwad Y., Saneja A.* (2021). Self-emulsifying formulations to augment therapeutic efficacy of nutraceuticals: From concepts to clinic. **Trends in Food Science & Technology**, 115, 347-365. https://doi.org/10.1016/j.tifs.2021.06.046 **(IF: 16.002)**

- Khan N., **Ruchika**, Dhritlahre R. K., Saneja A.* (2022). Recent advances in dual ligand targeted cancer therapy. **Drug Discovery Today,** 27, 2288-2299 https://doi.org/10.1016/j.drudis.2022.04.011 **(IF: 8.369)**

- Khan N., Bhardwaj V.K., **Ruchika**, Purohit R.*, and Saneja A.* (2023). Deciphering the interactions of genistein with β-cyclodextrin derivatives through experimental and microsecond timescale umbrella sampling simulations. **Journal of Molecular Liquids**, 374, 121295 https://doi.org/10.1016/j.molliq.2023.121295. **(IF: 6.633)**

- Sharma, P., **Ruchika,** Dhiman, P., Kumar, R., Saneja, A., & Singh, D. (2023). A solid dispersion of Citrus reticulata peel biowaste as an effective antiepileptic: Sustainable approach toward value addition and agro-industrial waste valorisation. **Journal of Drug Delivery Science and Technology**, 81, 104238 https://doi.org/10.1016/j.jddst.2023.104238 **(IF: 5.0).**

- **Ruchika**, Bhardwaj, N., Saneja., A*. Orally fast dissolving *α*-lipoic acid electrospun nanofibers mitigates lipopolysaccharide induced inflammation in RAW 264.7 macrophages. **Biomaterial Advances (Communicated)**

- **Ruchika**, Saneja A.* The dawning era of oral thin films for nutraceutical delivery: from laboratory to clinic. **Biotechnology Advances. (Communicated)**

Book chapters

- **Ruchika**, Saneja A*. (2021). Valorization of Sitosterol from Agricultural Waste as Therapeutic Agent. In: Rana A., Saneja A., Kumar S., Lichtfouse E (eds) Sustainable Agriculture Reviews 56. **Sustainable Agriculture Reviews,** vol 56. Springer, Cham. https://doi.org/10.1007/978-3-030-84405-9_5
- **Ruchika**, Dhritlahre R. K., Saneja A*. (2021) Nano-delivery of Bioactive Constituents from Apple Pomace. In: Rana A., Saneja A., Kumar S., Lichtfouse E (eds) Sustainable Agriculture Reviews 56. **Sustainable Agriculture Reviews**, vol 56. Springer, Cham. https://doi.org/10.1007/978-3-030-84405-9_3

First page of the papers are enclosed along with copies of two publications

JOURNAL OF AGRICULTURAL AND FOOD CHEMISTRY

pubs.acs.org/JAFC Article

R-α-Lipoic Acid Conjugated to D-α-Tocopherol Polyethylene Glycol 1000 Succinate: Synthesis, Characterization, and Effect on Antiseizure Activity

Ruchika, Savita Kumari, Poonam Dhiman, Damanpreet Singh, and Ankit Saneja*

Cite This: https://doi.org/10.1021/acs.jafc.2c01685 Read Online

ACCESS | Metrics & More | Article Recommendations | Supporting Information

ABSTRACT: α-Lipoic acid (LA), a dithiol micronutrient, acts as a vital cofactor in various cellular catabolic reactions and is also known as a universal antioxidant. The therapeutic efficacy of LA is compromised by a poor aqueous solubility as well as a short half-life. In the present study, LA was conjugated to D-α-tocopherol polyethylene glycol succinate (TPGS) using carbodiimideacid−alcohol coupling reaction. The synthesized conjugate (TPGS-LA) was characterized using ^{1}H and ^{13}C nuclear magnetic resonance (NMR), Fourier transform infrared spectroscopy (FT-IR), UV−vis spectroscopy, and matrix-assisted laser desorption/ionization time-of-flight mass spectrometry (MALDI-TOF MS). The TPGS-LA conjugate was demonstrated to be biocompatible and to have better anticonvulsion activity as compared to native LA in pentylenetetrazol (PTZ)-induced convulsions in zebrafish. Moreover, zebrafish larvae pretreated with TPGS-LA conjugate demonstrated a significant ($p < 0.05$) reduction of protein carbonylation levels and downregulation of *c-fos* expression during seizures as compared to native LA. Conclusively, the present findings demonstrate that the TPGS-LA conjugate can be a promising approach for the delivery of LA.

KEYWORDS: *lipoic acid, tocopherol poly(ethylene glycol) 1000 succinate, zebrafish, epilepsy, anticonvulsion activity*

INTRODUCTION

α-Lipoic acid (LA, 6,8-dithiooctanoic acid), an organosulfur compound belonging to the B-vitamins group, has a strong antioxidant potential.[1] Indeed, it is also recognized as a "universal antioxidant" reasoned to scavenge free radical species in direct (suppress and scavenge radical species directly) and indirect (initiating the transcription of antioxidant enzymes via the nucleus) ways. Moreover, it is effective in the prevention or treatment of various diseases such as liver,[2] cardiovascular,[3] diabetes,[4] and Alzheimer's[5] diseases. A recent study found that LA dramatically reduced the occurrence of epileptic seizures and alleviated the behavioral dysfunction in rats induced by pentetrazol via an Nrf2 pathway.[6] It is also reported that a deficiency of LA inside the body may lead to early infantile epileptic encephalopathy.[7] Despite its tremendous therapeutic potential, LA is associated with poor aqueous solubility, short half-life (~30 min), and poor bioavailability (about 30%) which ultimately limits its therapeutic efficacy.[8]

To overcome these limitations, much attention has been given to the development of LA delivery systems such as the self-emulsifying delivery system (SEDDS),[9] nanoemulsions,[10] polymeric nanoparticles,[11] lipid nanoparticles,[12] etc. However, one of the most promising approaches to tackle these challenges is to explore polymer conjugates of these therapeutic agents which also have the ability to self-assemble into nanostructures. In this regard, a nonionic, amphiphilic self-assembling tocopherol polyethylene glycol succinate (TPGS) polymer is gaining tremendous attention for the delivery of therapeutic agents because of its GRAS (generally recognized as safe) status and its use as an absorption enhancer and stabilizer in various formulations. The conjugation of TPGS with several drugs such as paclitaxel,[13] doxorubicin,[14] cantharidin,[15] and gemcitabine[16] has demonstrated better therapeutic efficacy as compared to their native counterparts. More interestingly, the surface modifications of nanoformulations with TPGS and its derivatives have been demonstrated to overcome biological barriers including the blood−brain barrier (BBB) by enhancing uptake of these formulations.[17] On the other side, zebrafish experimental models are now receiving tremendous attention to explore the pathophysiology and pharmacology of neurological diseases such as epilepsy,[18] Parkinson's disease,[19] and motor neuron diseases.[20]

Therefore, considering these aspects, in the present investigation, we have conjugated LA with TPGS via an ester bond. The characterization of the synthesized conjugate was executed using different analytical techniques such as ^{1}H NMR, ^{13}C NMR, and FT-IR. Molecular weights of TPGS and the synthesized TPGS-LA conjugate have been analyzed using matrix-assisted laser desorption/ionization time-of-flight mass spectrometry (MALDI-TOF MS) . The biocompatibility of the synthesized conjugate has been assessed using zebrafish embryos/larvae. The antiepileptic evaluation of the TPGS-LA conjugate was performed using pentylenetetrazol (PTZ)-

Received: March 9, 2022
Revised: May 25, 2022
Accepted: June 3, 2022

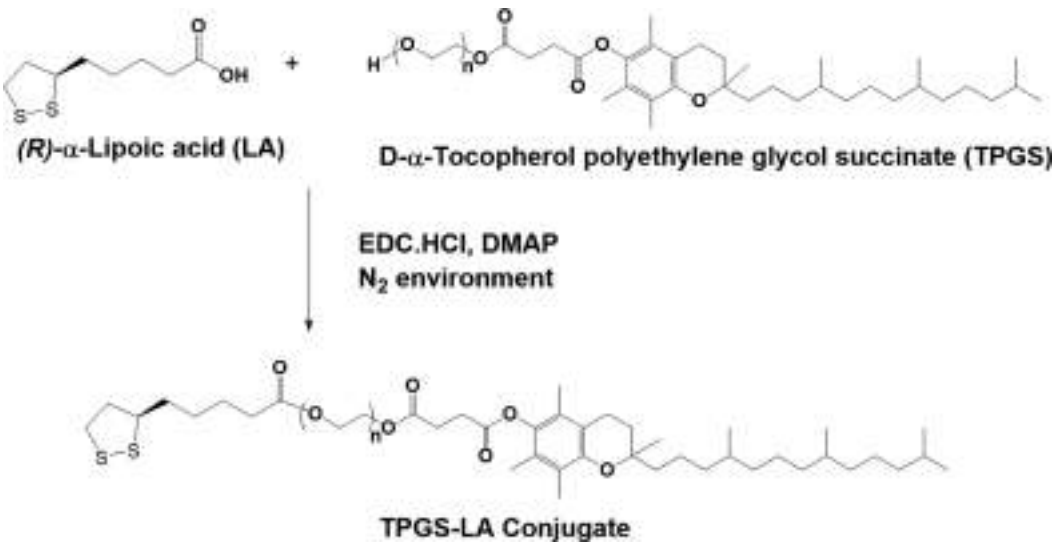

Figure 1. Synthetic scheme for D-α-tocopherol polyethylene glycol succinate 1000 (TPGS)-lipoic acid (TPGS-LA) conjugate. EDC·HCl: 1-Ethyl *N*-3-(3-(dimethylamino)propyl)) carbodiimide hydrochloric acid. DMAP: 4-(Dimethylamino) pyridine.

induced convulsions in zebrafish larvae. Finally, the effect of the LA and TPGS-LA conjugate treatment on the protein carbonylation and expression of *c-fos*, a transsynaptic marker of neuronal activity in the zebrafish larval brain, was assessed.

MATERIALS AND METHODS

Materials. D-α-Tocopherol polyethylene glycol 1000 succinate (TPGS), pentylenetetrazol (PTZ), anhydrous dichloromethane (DCM), 4-(dimethylamino) pyridine (DMAP), a Pur-A-Lyzer dialysis kit (MWCO 1 kDa), and TRIZOL reagent were purchased from Sigma-Aldrich. (*R*)-α-Lipoic acid (LA) was purchased from Tokyo Chemical Industry (TCI). 1-ethyl *N*-3-(3-(dimethylamino)propyl) carbodiimide hydrochloric acid (EDC·HCl) was procured from HiMedia Laboratories. A Verso cDNA synthesis kit and GoTaq qPCR Master Mix were procured from Thermo Fisher Scientific and Promega, respectively. All other solvents and reagents used were of analytical grade.

Synthesis of TPGS-(R)-α-Lipoic Acid Conjugate (TPGS-LA). TPGS-Lipoic acid (TPGS-LA) conjugate was synthesized via a single-step carbodiimide acid−alcohol coupling reaction by using EDC·HCl as a coupling agent and DMAP as a base[14,21] (Figure 1). In a 50 mL round-bottom flask, LA (3 equiv), EDC·HCl (3 equiv), and DMAP (0.1 equiv) were dissolved in 10 mL of anhydrous dichloromethane (CH_2Cl_2) for 20 min under a N_2 environment in an ice bath. To the above reaction mixture, TPGS (500 mg, 0.33 mM, 1 equiv) in 5 mL of dichloromethane was added, and the reaction was continued with stirring for 36 h under a N_2 environment at room temperature (RT). The resultant product was dried under reduced pressure, dissolved in ethanol, and dialyzed (via a Pur-A-Lyzer dialysis kit, MWCO 1 kDa) in two steps for 72 h, first against 70% ethanol for 24 h and then against deionized water for 48 h to remove unreacted LA and side products. The purified product was lyophilized (Labconco FreeZone freeze-dryer) and stored at −20 °C for further use.

Characterization of TPGS-LA Conjugate. The conjugation of LA with TPGS was analyzed using NMR, FT-IR, and MALDI. ^{1}H NMR (600 MHz) and ^{13}C NMR (151 MHz) spectra were recorded for LA, TPGS, and TPGS-LA conjugate by an NMR spectrometer (AV-600, Bruker) using $CDCl_3$ as the solvent. The FT-IR spectra were recorded using a PerkinElmer FT-IR spectrometer in chloroform over the range 4000−500 cm^{-1}. The mass spectrum of TPGS and TPGS-LA was obtained by MALDI-TOF (Bruker Ultraflex TOF/TOF), ranging from 1000 to 2400 Da. UV spectra of synthesized TPGS-LA conjugate were also analyzed using a GENESYS 180 UV−vis spectrophotometer.

Zebrafish Husbandry and Embryo Culture. A wild type zebrafish (*Danio rerio*) strain was reared in a standalone system (Tecniplast, Buguggiate, Varese, Italy) maintaining the standard aquatic environment, proper aeration, and four-stage filtration system. Housing tanks were maintained at controlled aquatic conditions of 7.0−7.5, 26−28 °C, and 400−600 μS values for the pH, temperature, and conductivity of the system water, respectively. Zebrafish were fed a live diet (*Artemia*, Inve Aquaculture, Inc., Salt Lake City, UT) two times a day with a 14 h light and 10 h dark cycle. For breeding purposes, special breeding tanks were placed at a 2:1 female to male ratio, and thereafter, healthy eggs were collected in a glass Petri dish and cleaned thrice with system water. After cleaning, eggs were raised in a biological oxygen demand (BOD) incubator maintained at 28.5 ± 0.5 °C with the water changed daily. The experimental protocol was approved by the Institutional (CSIR-IHBT) Animal Ethics Committee (IAEC).

Evaluation of Biocompatibility of TPGS-LA on Zebrafish. The biocompatibility of synthesized TPGS-LA conjugate was investigated by analyzing the complete embryonal development of zebrafish embryos up to 120 h postfertilization (hpf).[22] In brief, 4 hpf embryos were collected and cleaned thrice with system water carefully to avoid any contamination. Embryos were randomly divided into four groups [Naïve vehicle (NV) and three groups of TPGS-LA conjugate] with 20 embryos in each group. Naïve group embryos were reared in 2 mL of system water in a 24-well plate with 3 embryos in each well, whereas treatment group embryos were cultured in system water with concentrations of 5, 10, and 20 μM TPGS-LA conjugate (equivalent to LA) in the BOD incubator maintained at 28.5 ± 0.5 °C. The solution was changed thrice in 24 h, and all developmental stages were observed under a Nikon stereomicroscope (SMZ 800N, Nikon, Tokyo, Japan). Numbers of surviving and hatching embryos were observed carefully, and survival and hatching rate percentages were calculated using the following equations:

$$\text{survival rate of embryos (\%)} = \frac{\text{number of healthy embryos}}{\text{total number of embryos}} \times 100$$

$$\text{hatching rate of embryos (\%)} = \frac{\text{number of hatched embryos}}{\text{total number of embryos}} \times 100$$

Evaluation of Seizure Latency and Locomotor Activity Tests on PTZ-Induced Seizures. The PTZ drug, a common chemo-convulsant, acts as an antagonist to the γ-aminobutyric acid (GABA) receptor and induces seizures. PTZ-induced seizures in the zebrafish larvae manifest three different stages, i.e., stage I, hyperactivity stage, characterized by an increase in speed and abnormal swimming

https://doi.org/10.1021/acs.jafc.2c01685
J. Agric. Food Chem. XXXX, XXX, XXX−XXX

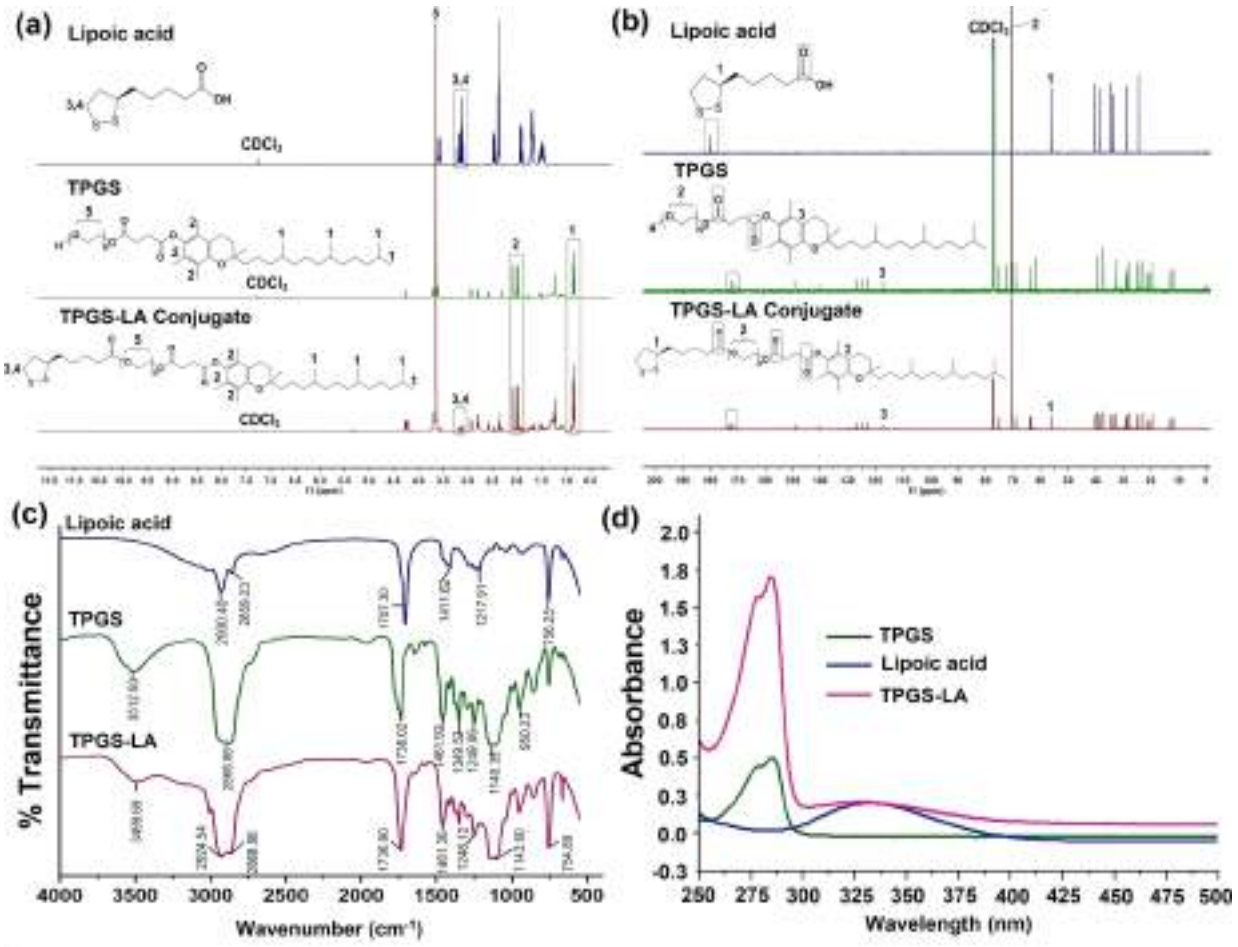

Figure 2. (a) ^{1}H (600 MHz) and (b) ^{13}C NMR (151 MHz) spectra of native lipoic acid (LA), TPGS, and TPGS-LA conjugate in deuterated chloroform ($CDCl_3$). The NMR spectrum of TPGS-LA conjugate demonstrated peaks of both TPGS and LA. The peak in the ^{13}C NMR at δ 180 ppm (due to the carboxylic group of lipoic acid) was shifted upfield to δ 173 ppm in TPGS-LA conjugate due to ester bond formation. (c) Stacked Fourier transform-infrared (FT-IR) spectra of LA, TPGS, and TPGS-LA with a scanning range from 4000 to 500 cm^{-1}. (d) UV−vis spectra of LA, TPGS, and TPGS-LA conjugate.

pattern; stage II, whirlpool stage exhibiting circular whirlpool-like movements; and stage III, clonus-like seizure stage with strong body twitching movements resulting in a sloping position accompanied by complete loss of posture.[22] Concisely, 7 dpf larvae were randomly divided into four groups, LA1, LA5, LA10, and TPGS-LA, with 10 larvae in each group, and were incubated for 1 h in 1, 5, and 10 μM concentrations of LA and a 5 μM concentration (equivalent to LA) of TPGS-LA conjugate, respectively (dpf, days postfertilization). After incubation, each larva was gently transferred to the well [3.5 cm (diameter), 2 cm (depth)] containing 3.5 mL of 8 mM PTZ solution maintained at 28 ± 0.5 °C, and latency to first clonus seizures (stage III) was noted with a fixed upper cut-off timing of 15 min. Furthermore, distance traveled and mean velocity as an index of hyperactive response were recorded for an initial 5 min. For recording and eliminating human error, a camera (c922 Pro Stream, Logitech Asia Pacific Ltd., Hong Kong) connected with a video tracking system (SMART V.3.0.Panlab Barcelona) was used. Naïve vehicle (NV) and the PTZ-treated group were also recorded separately.

Real-Time Quantitative PCR to Assess the Modulation of the mRNA Levels of *c-fos*. c-*fos* gene expression was analyzed in treated as well as nontreated 7 dpf larva as reported earlier.[22] In brief, 7 dpf zebrafish larvae were randomly categorized in four groups, namely, naïve control (NV; with system water), vehicle control (PTZ), lipoic acid (LA10; 10 μM), and TPGS-LA conjugate (TPGS-LA; 5 μM equivalent to LA). Every group had three independent sets of 20 larvae each.[23] After incubation, all groups were exposed to 8 mM PTZ solution for 15 min separately, except the naïve group. The exposed larvae were sacrificed, and RNA isolation was performed by using TRIZOL reagent (Sigma-Aldrich). The isolated RNA sample was further processed into cDNA using the Verso cDNA synthesis kit (Thermo Fisher Scientific) as per the instructions provided by the manufacturer. Further, the quantitative real-time polymerase chain reaction (AriaMx Real-Time PCR, Agilent Technologies) was carried out by using GoTaq qPCR Master Mix (Promega). Primers were designed via Primer3 Input (v.0.4.0) software and have sequences *eef1a1b*, [F, TATCTCAAAGAACGGGCAAA; R, TTCACAATC-TCCTCATAGCG]; and *c-fos*, [F, TTACCGGTGCTAGATTTGTT; R, ATTCACACGTTCAGAAATCC]. *eef1a1b* was used as an internal control for qRT PCR analysis. The 2^ddCT method was used to analyze the gene expression, and each value was expressed relative to the naïve control.

Protein Carbonylation Assay to Assess the Modulation of Oxidative Stress Levels. The leftover supernatant following the RNA isolation was used for protein isolation. The DNA was first isolated from the leftover solution to avoid nucleic acid contamination as described earlier.[24] Further, chilled isopropanol was added in the supernatant collected after DNA isolation for precipitation, followed by 10 min of incubation and centrifugation at 12 000*g* for 5 min at 4 °C. The obtained protein pellet was washed thrice with 0.3 M guanidine hydrochloride solution (in 95% ethanol) and finally with absolute ethanol. The protein pellet was air-dried, resuspended in rehydration buffer, and stored at −20 °C for further use. Protein concentration was analyzed by Bradford assay.[25] For the determination of levels of protein carbonylation due to oxidative stress in

https://doi.org/10.1021/acs.jafc.2c01685
J. Agric. Food Chem. XXXX, XXX, XXX−XXX

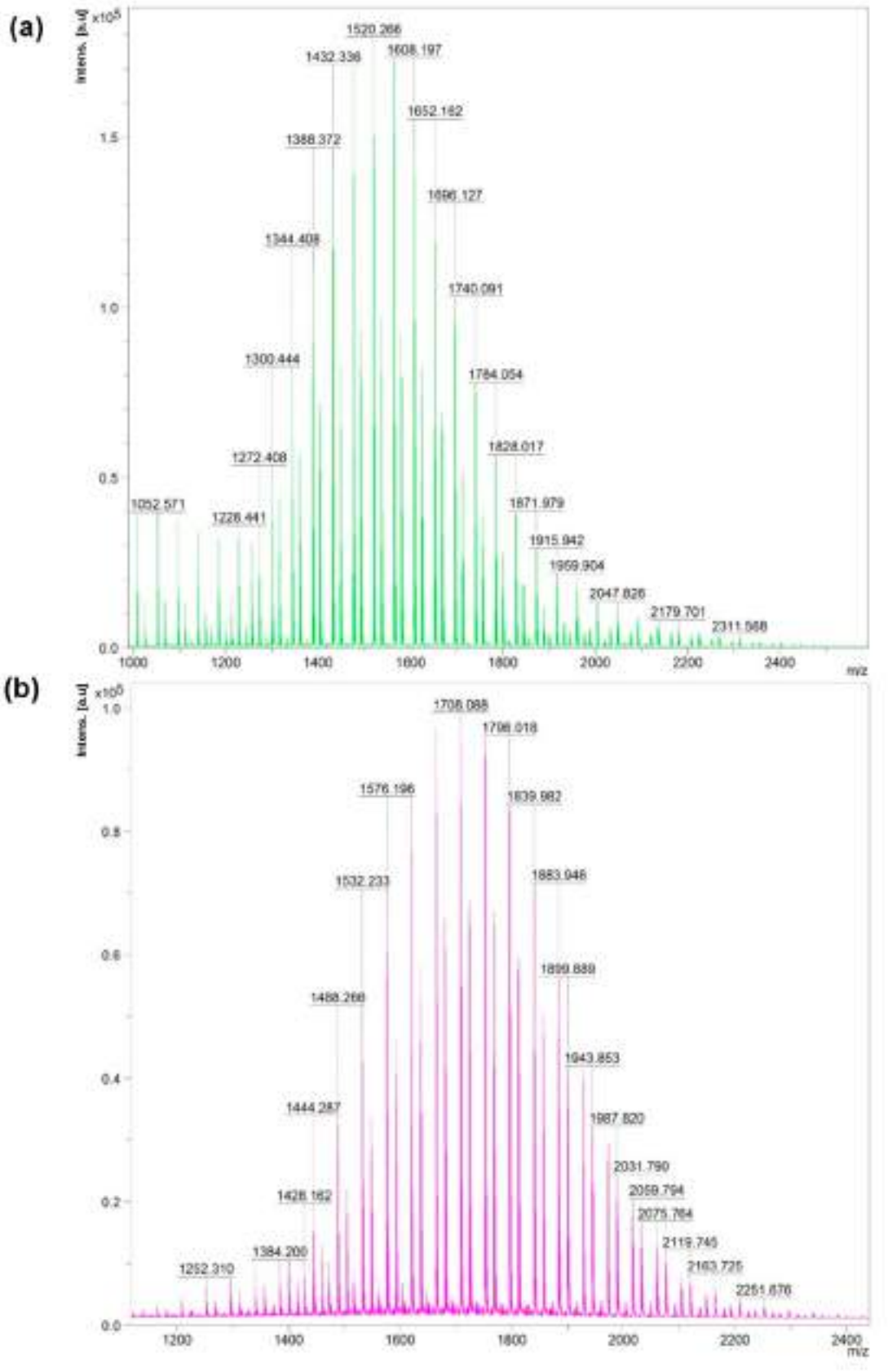

Figure 3. MALDI-TOF spectra of (a) TPGS and (b) TPGS-LA conjugate with a scanning range from 1000 to 2400 Da. Each peak of TPGS-LA conjugate spectra shifted by a common mass factor of 188 Da which corresponds to the mass of one LA molecule covalently conjugated with one molecule of TPGS.

https://doi.org/10.1021/acs.jafc.2c01685
J. Agric. Food Chem. XXXX, XXX, XXX−XXX

larvae, the most frequently used protein carbonylation spectrophotometric assay was performed. Briefly, an equal volume of 2,4-dinitrophenylhydrazine (DNPH) (10 mM in 0.5 M H_3PO_4) and protein with an equivalent concentration from all samples were mixed and incubated for 15 min in the dark. Further, 50% w/v trichloroacetic acid solution was added to the mixture for the precipitation of DNPH adduct, and the mixture was incubated at 20 °C for 15 min. The resultant solution was centrifuged, and the DNPH adduct pellet was collected, washed thrice with a mixture of binary solvents [ethanol/ethyl acetate (1:1 v/v)], and solubilized in 6 M guanidine hydrochloride. The absorbance was recorded at 370 nm, and quantification was performed with a molar coefficient of 22 000 M^{-1} cm^{-1}.

STATISTICS

The results of latency to clonus-like seizures, total distance traveled, mean speed, protein carbonylation content, and relative mRNA levels were represented as mean ± standard error. The level of significance at $p < 0.05$ among different groups was analyzed by a one-way analysis of variance followed by Tukey's post hoc test with SigmaStat statistical software.

RESULTS AND DISCUSSION

Synthesis and Characterization of TPGS-LA Conjugate. In this study, we have explored the polymer drug conjugation approach to augment the therapeutic efficacy of α-lipoic acid. TPGS-LA conjugate was synthesized via esterification between the carboxylic acid group of LA with the hydroxyl group of TPGS. Excessive LA was used in order to achieve a complete reaction as it is easier to separate the low-molecular-weight LA from the large molecular TPGS-LA conjugate. The synthesized TPGS-LA conjugate was confirmed by ^1H and ^{13}C NMR spectroscopy (Figure 2a,b). The ^1H NMR spectrum of TPGS demonstrated characteristic peaks of methylene protons in vitamin E at δ 0.86 ppm and CH_2—CH_2—O— (PEG chain) protons at δ 3.6 ppm[13,26] (Figure 2a). Similar peaks were observed in the ^1H NMR spectrum of TPGS-LA conjugate along with peaks corresponding to LA at δ 3.11−3.18 ppm, thus confirming the successful reaction between TPGS and LA.[27] Further, ^{13}C NMR of TPGS-LA conjugate shows the peaks of both LA and TPGS (Figure 2b). The spectrum of TPGS demonstrated peaks at δ 171 and δ 172 ppm corresponding to its two carbonyl (—C═O) groups. The peak in the ^{13}C NMR results at δ 180 ppm (because of the carboxylic group of LA) was shifted upfield to δ 173 ppm in TPGS-LA conjugate due to ester bond formation, and a total of three peaks at the δ 171, δ 172, and δ 173 ppm region were observed, representing three carbonyl groups (two of TPGS and one of LA).[28] Moreover, from the integration in ^1H NMR peaks, it was concluded that approximately 95% of LA is conjugated with TPGS.

The FT-IR spectra of native TPGS shows a characteristic band at 1738.02 cm^{-1} which attributes to the carbonyl group (C═O) present in the TPGS.[16] While comparing FT-IR spectra of LA with those of TPGS-LA, a shifting and strong absorption of the carbonyl band from 1707.30 to 1736.90 cm^{-1} was observed, confirming the replacement of the carboxyl group with the ester moiety, which thus provides evidence of ester bond formation between TPGS and LA.[29] Additionally, peaks at 1143.60 and 2924.54 cm^{-1} correspond to —COO— and —CH_2 group stretching in TPGS, respectively (Figure 2c). UV−vis spectra of conjugate were also recorded which reveal the appearance of both of the peaks corresponding to the λ_{max} of both TPGS (λ_{max} 280 nm) as well as LA (λ_{max} 332 nm) which is usually observed in polymer drug conjugates[30] (Figure 2d).

The conjugation of LA with TPGS was also confirmed using MALDI-TOF MS (Figure 3). The MALDI spectra of TPGS and TPGS-LA conjugate both demonstrated a peak variation of 44 Da between each peak because of CH_2CH_2O repeating monomeric units of PEG. LA has a mass of 206.32 Da, and its covalent linkage with TPGS should demonstrate a mass increase of about 188 Da in its oligomeric structure as compared to TPGS, demonstrating the successful conjugation of LA with TPGS (see Table S1). For instance, the peak of TPGS at 1520 has been shifted to 1708, which is equivalent to one LA molecule.

Biocompatibility of TPGS-LA Conjugate on Zebrafish. The zebrafish is now a renowned model for assessing the biocompatibility of therapeutic agents because of its rapid and *ex utero* development which is ideally suited for the screening of potent molecules.[31] Therefore, the biocompatibility of synthesized TPGS-LA conjugate was assessed in zebrafish embryos, and any maltransformations/lethality was observed until 120 hpf. The end point includes coagulation of embryos; loss of heartbeat; delayed hatching; deformation in the tail, eyes, and head; and reduced pigmentation.[32] One distinctive aspect of zebrafish development is their sensitivity toward administered solutions in terms of timing and extent of hatching (which occurs around 2−3 dpf). Based on these aspects, survival, hatching rate, and overall embryonic development of larvae were monitored[33] (see the Supporting Information, Figures S1 and S2). Our results demonstrated that TPGS-LA conjugate imposed negligible variations in the morphology as well as the overall activity of larvae up to a 20 μM concentration (equivalent to LA; Figure 4).

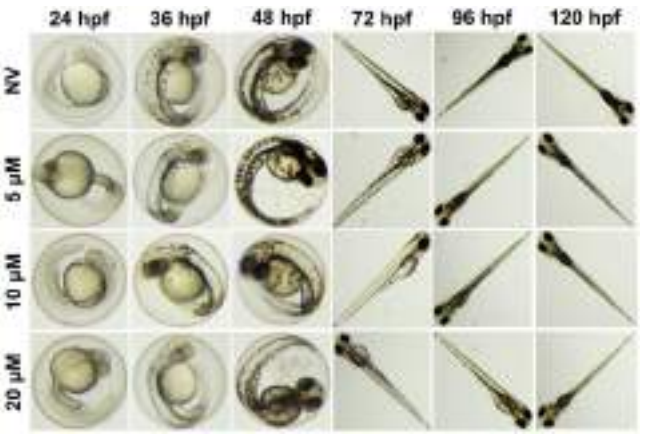

Figure 4. Photographic representation of the embryonic development of zebrafish upon treatments with different concentrations of TPGS-LA conjugate (5, 10, and 20 μM equivalent to LA) in system water over a period from 24 to 120 hpf.

Effects of TPGS-LA Conjugate on Behavioral Seizure Response Post-PTZ. PTZ is a chemical agent that causes seizures in animals by blocking the functioning of chloride channels via binding to the $GABA_A$ receptor.[34] PTZ is considered to be a potent chemoconvulsant commonly used in the development of experimental seizure models.[35] Zebrafish larvae also behave identical to rodents when exposed to PTZ and exhibit concentration-dependent convulsing activity.[36] Here, we have used an 8 mM concentration of PTZ

https://doi.org/10.1021/acs.jafc.2c01685
J. Agric. Food Chem. XXXX, XXX, XXX−XXX

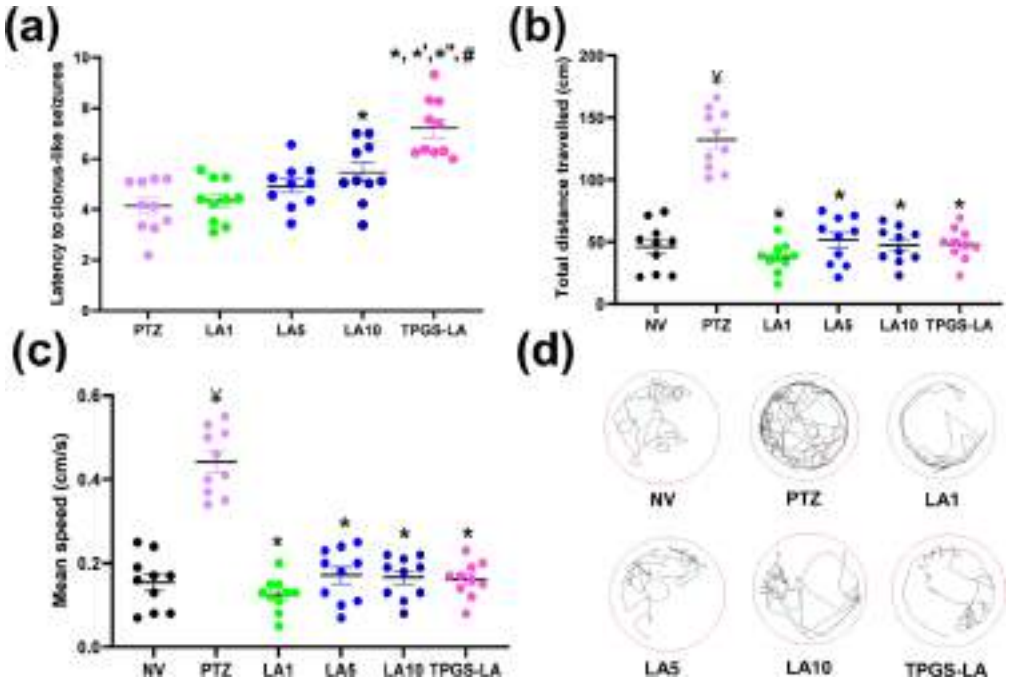

Figure 5. Effect of LA and TPGS-LA conjugate on (a) latency to clonus-like seizure and PTZ- induced hyperactivity as (b) total distance traveled in cm and (c) mean speed in cm/s. (d) Movement track of 7 dpf larva during PTZ exposure for 5 min. $^{¥}p < 0.05$ as compared to NV, $^{*}p < 0.05$ as compared to PTZ, $^{*'}p < 0.05$ as compared to LA1, $^{*''}p < 0.05$ as compared LA5, and $^{\#}p < 0.05$ as compared LA10. NV: 7 dpf larvae incubated in system water, not exposed to PTZ. PTZ: system-water-incubated 7 dpf larva exposed to PTZ (8 mM). LA1: lipoic acid (1 μM)-incubated larva exposed to PTZ. LA5: lipoic acid (5 μM)-incubated larva exposed to PTZ. LA10: lipoic acid (10 μM)-incubated larva exposed to PTZ. TPGS-LA: TPGS-LA (equivalent to 5 μM lipoic acid)-incubated larva exposed to PTZ.

which potentially induced a hyperactive response within the first few minutes of exposure followed by severe seizures to loss of posture as time passed. It has been established that the pretreatment of any antiepileptic compound or entity decreases the PTZ-induced hyperactive response and increases the time for the arrival of clonus-like seizures in the respective animal model.[37]

As seizures or convulsions are the most prominent and distinct symptom of epilepsy, latency in the arrival of clonus-like seizures was recorded to evaluate the pretreatment antiepileptic potential of synthesized TPGS-LA conjugate. Preincubated TPGS-LA conjugate (5 μM equivalent to LA) larvae and LA10 (10 μM) exhibited an increment in latency to PTZ-induced convulsions in comparison to PTZ and other LA groups (LA1 and LA5; Figure 5a). There was a significant ($p < 0.05$) increase in timing of clonus-like seizures in TPGS-LA conjugate (7.5 min) as compared to the PTZ group (4.1 min) and LA groups (LA1, 4.5 min; LA5, 4.9 min; and LA10, 5.53 min) whereas differences among LA1 and LA5 groups in comparison to the PTZ group were observed to be insignificant.

Here, PTZ potentially induces a hyperactive response in larvae exposed with PTZ as compared to the naïve control as there was a significant ($p < 0.05$) difference in total distance traveled in the PTZ group in comparison to the naïve control (Figure 5b). However, preincubation with TPGS-LA at 5 μM (equivalent to LA) and LA at 1, 5, and 10 μM demonstrated a significant decrease in total distance traveled in contrast to the PTZ group ($p < 0.05$).

A similar trend was observed in the swimming pattern and speed in all groups. The PTZ group showed a marked increase in the mean speed of larvae at a significance level of $p < 0.05$ as compared to the naïve group. A significant ($p < 0.05$) decrease in speed was observed in all treatment groups (LA1, LA5, LA10, and TPGS-LA) in contrast to the PTZ group (Figure 5c).

Increased speed and locomotor activity are the first sign of seizurelike behavior in epileptic zebrafish. Thus, suppression and regulation of these parameters can indicate the antiepileptic activity of the compound.[6] Here, we observed a similar pattern, as PTZ-treated larvae demonstrated increased distance traveled and mean speed, whereas the treatment group suppresses all of these behaviors. All of these findings align with previously reported findings that any antiepileptic entity potentially improves and regulate seizure-associated indicators and also delays the onset of seizures in *in vivo* models and also in humans.[22,38,39] Consequently, the results of the current study suggest that TPGS-LA conjugate significantly decreased the hyperactive response (total distance traveled and mean speed) and also exhibited increased latency to clonus-like seizures at a 5 μM concentration in comparison to both PTZ and LA (1, 5, and 10 μM concentrations) groups.

Effect of TPGS-LA Conjugate on Protein Carbonylation. Epilepsy is a dynamic process of frequent neuronal deaths which may be due to several factors. One of the most common factors is oxidative stress as the brain is an organ that is highly susceptible to oxidative stress, and high levels of intracellular calcium during seizures can induce free radical species.[39] Oxidative stress results in oxidation of proteins, lipids, and nucleotides which has a great impact on pathophysiological conditions. Protein carbonylation is considered as the hallmark of oxidative stress in the brain. Thus, the level of protein carbonylation was determined by using a DNPH-based protein carbonylation assay. This involves the formation of stable dinitrophenyl (DNP) hydrazone after the reaction with carbonyl group of proteins.[40] A significant

https://doi.org/10.1021/acs.jafc.2c01685
J. Agric. Food Chem. XXXX, XXX, XXX−XXX

increase ($p < 0.05$) in carbonylation of protein was observed in the PTZ-treated group of larvae in comparison to the naïve group. TPGS-LA-treated groups exhibited a marked decrease in protein carbonylation levels in comparison to PTZ (Figure 6a). However, no significant difference in protein carbonylation was observed between PTZ and LA10 groups. These results indicated that TPGS-LA at a 5 μM concentration significantly reduces the formation of carbonylated protein via reducing oxidative stress in comparison to the native LA at 10 μM.

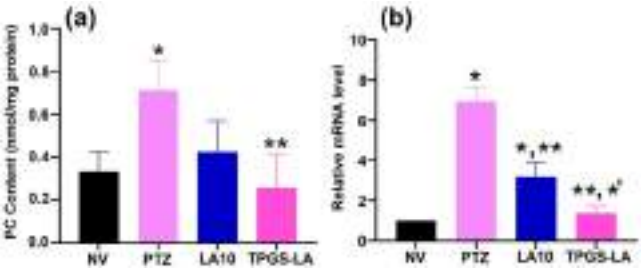

Figure 6. Effect of LA and TPGS-LA on (a) protein carbonylation levels in larvae exposed to PTZ and (b) *c-fos* expression of larvae exposed to PTZ. *$p < 0.05$ as compared to NV, **$p < 0.05$ as compared to PTZ, and *'$p < 0.05$ as compared to LA10. NV: 7 dpf larvae incubated in system water, not exposed to PTZ. PTZ: system-water-incubated 7 dpf larva exposed to PTZ (8 mM). LA10: lipoic acid (10 μM)-incubated larva exposed to PTZ. TPGS-LA: TPGS-LA conjugate (5 μM)-incubated larva exposed to PTZ.

Effect of TPGS-LA Conjugate on the mRNA Expression of *c-fos*. *c-fos* is considerably used to detect aberrant neuronal activation and is proposed to be positively related with level of convulsions as it is upregulated in the case of seizures, inflammation, and injury.[37,41] It plays a significant role in various neuronal physiological processes and is also related to neuronal malfunctioning and cell death in excitotoxicity conditions.[42] To assess the effect of pretreatment of TPGS-LA conjugate (5 μM equivalent to LA) and LA (10 μM) on *c-fos* expression, *c-fos* mRNA expression was assessed via quantitative PCR. Our results revealed that PTZ significantly upregulated *c-fos* expression as compared to the naive control, whereas TPGS-LA conjugate significantly downregulated the *c-fos* expression in comparison to both PTZ and LA groups (Figure 6b).

Our results are in corroboration with the earlier finding on PTZ-induced upregulation of *c-fos* expression in 7 dpf zebrafish larvae and also in rodent models.[38,43] It is well-reported that PTZ exposure increases *c-fos* expression by several fold in different regions of the zebrafish larval brain, and the antiseizure entity reduces its expression.[22,38,44] Altogether, our results demonstrated an ameliorated effect of TPGS-LA conjugate as compared to native LA in terms of latency in seizures, reduced hyperactivity, and downregulation of *c-fos* gene expression which are the markers of epilepsy, thus reflecting an enhanced protective effect of TPGS-LA as compared to native LA in PTZ-induced convulsions.

In this investigation, we have synthesized and characterized TPGS-LA conjugate via the conjugation of the LA carboxylic group with the hydroxyl group of TPGS. Further, the synthesized TPGS-LA conjugate exhibited an enhanced antiseizure activity in comparison to LA via increasing latency in clonus like seizures, a decreased hyperactive response of zebrafish larvae, and a reduction in oxidative stress. Moreover, conjugate also potentially downregulates *c-fos* expression (a marker of neuronal activity) in PTZ-induced convulsion in larvae. In summary, our findings concluded that TPGS-Lipoic acid conjugate can be a promising approach for ameliorating the therapeutic efficacy of lipoic acid.

■ ASSOCIATED CONTENT

Supporting Information

The Supporting Information is available free of charge at https://pubs.acs.org/doi/10.1021/acs.jafc.2c01685.

Details of the experimental molecular weight of TPGS-LA conjugate recorded by MALDI-TOF and readouts of survival and hatching rates of the biocompatibility experiment after the exposure of TPGS-LA conjugate over a period of 5 days (PDF)

■ AUTHOR INFORMATION

Corresponding Author

Ankit Saneja − *Formulation Laboratory, Dietetics and Nutrition Technology Division, CSIR−Institute of Himalayan Bioresource Technology, Palampur 176061 Himachal Pradesh, India; Academy of Scientific and Innovative Research (AcSIR), Ghaziabad 201002 Uttar Pradesh, India;* orcid.org/0000-0002-2423-4704; Phone: 91-1894-233339; Email: ankitsaneja@ihbt.res.in; Fax: +91-1894-230433

Authors

Ruchika − *Formulation Laboratory, Dietetics and Nutrition Technology Division, CSIR−Institute of Himalayan Bioresource Technology, Palampur 176061 Himachal Pradesh, India; Academy of Scientific and Innovative Research (AcSIR), Ghaziabad 201002 Uttar Pradesh, India*

Savita Kumari − *Pharmacology and Toxicology Laboratory, Dietetics and Nutrition Technology Division, CSIR−Institute of Himalayan Bioresource Technology, Palampur 176061 Himachal Pradesh, India; Academy of Scientific and Innovative Research (AcSIR), Ghaziabad 201002 Uttar Pradesh, India*

Poonam Dhiman − *Pharmacology and Toxicology Laboratory, Dietetics and Nutrition Technology Division, CSIR−Institute of Himalayan Bioresource Technology, Palampur 176061 Himachal Pradesh, India; Academy of Scientific and Innovative Research (AcSIR), Ghaziabad 201002 Uttar Pradesh, India*

Damanpreet Singh − *Pharmacology and Toxicology Laboratory, Dietetics and Nutrition Technology Division, CSIR−Institute of Himalayan Bioresource Technology, Palampur 176061 Himachal Pradesh, India; Academy of Scientific and Innovative Research (AcSIR), Ghaziabad 201002 Uttar Pradesh, India*

Complete contact information is available at: https://pubs.acs.org/10.1021/acs.jafc.2c01685

Funding

The authors acknowledge financial assistance from Science and Engineering Research Board (SERB), New Delhi, for the GAP-270 project (File SRG/2020/000141) and Council of Scientific and Industrial Research (CSIR), New Delhi for MLP-204 project.

Notes

The authors declare no competing financial interest.

■ ACKNOWLEDGMENTS

The authors are grateful to the Director, CSIR-Institute of Himalayan Bioresource Technology, for his continuous support and encouragement. R. acknowledges Council of Scientific and Industrial Research (CSIR), New Delhi, for providing a fellowship (File 31/054(0163)/2020-EMR-I). P.D. is grateful to the CSIR, New Delhi, India, for granting a Junior Research Fellowship (File 31/054(0158)/2020-EMR-I). The Authors acknowledge the central instrumentation facility at CSIR—Indian Institute of Integrative Medicine (IIIM) Jammu for carrying out FT-IR analyses. This Article is institutional communication 4953.

■ ABBREVIATIONS USED

LA, lipoic acid; TPGS, D-α-tocopherol poly(ethylene glycol) 1000 succinate; PTZ, pentylenetetrazol

■ REFERENCES

(1) Salehi, B.; Berkay Yılmaz, Y.; Antika, G.; Boyunegmez Tumer, T.; Fawzi Mahomoodally, M.; Lobine, D.; Akram, M.; Riaz, M.; Capanoglu, E.; Sharopov, F. Insights on the use of α-lipoic acid for therapeutic purposes. *Biomolecules* **2019**, *9* (8), 356.

(2) Yang, Y.; Li, W.; Liu, Y.; Sun, Y.; Li, Y.; Yao, Q.; Li, J.; Zhang, Q.; Gao, Y.; Gao, L. Alpha-lipoic acid improves high-fat diet-induced hepatic steatosis by modulating the transcription factors SREBP-1, FoxO1 and Nrf2 via the SIRT1/LKB1/AMPK pathway. *Journal of nutritional biochemistry* **2014**, *25* (11), 1207−1217.

(3) Jamshidi, K.; Abdollahzad, H.; Nachvak, M.; Rezaei, M.; Golpayegani, M. R.; Zahabi, E. S. Effects of Alpha-Lipoic Acid Supplementation on Cardiovascular Disease Risk Factors in β-Thalassemia Major Patients: A Clinical Trial Crossover Study. *Journal of Blood Medicine* **2020**, *11*, 131.

(4) Laher, I. Diabetes and alpha lipoic acid. *Frontiers in pharmacology* **2011**, *2*, 69.

(5) Fava, A.; Pirritano, D.; Plastino, M.; Cristiano, D.; Puccio, G.; Colica, C.; Ermio, C.; De Bartolo, M.; Mauro, G.; Bosco, D. The effect of lipoic acid therapy on cognitive functioning in patients with Alzheimer's disease. *Journal of neurodegenerative diseases* **2013**, *2013*, 1.

(6) Cheng, Y.; Luo, F.; Zhang, Q.; Sang, Y.; Chen, X.; Zhang, L.; Liu, Y.; Li, X.; Li, J.; Ding, H. α-Lipoic acid alleviates pentetrazol-induced neurological deficits and behavioral dysfunction in rats with seizures via an Nrf2 pathway. *RSC Adv.* **2018**, *8* (8), 4084−4092.

(7) Stowe, R. C.; Sun, Q.; Elsea, S. H.; Scaglia, F. LIPT1 deficiency presenting as early infantile epileptic encephalopathy, Leigh disease, and secondary pyruvate dehydrogenase complex deficiency. *American Journal of Medical Genetics Part A* **2018**, *176* (5), 1184−1189.

(8) Teichert, J.; Kern, J.; Tritschler, H.; Ulrich, H.; Preiss, R. Investigations on the pharmacokinetics of alpha-lipoic acid in healthy volunteers. *International journal of clinical pharmacology and therapeutics* **1998**, *36* (12), 625−628.

(9) Banik, S.; Halder, S.; Sato, H.; Onoue, S. Self-emulsifying drug delivery system of (R)-α-lipoic acid to improve its stability and oral absorption. *Biopharmaceutics & Drug Disposition* **2021**, *42* (5), 226−233.

(10) Çoban, Ö.; Yıldırım, S.; Bakır, T. Alpha-Lipoic Acid and Cyanocobalamin Co-Loaded Nanoemulsions: Development, Characterization, and Evaluation of Stability. *Journal of Pharmaceutical Innovation* **2021**, in press. DOI: 10.1007/s12247-020-09531-4

(11) Gogoi, P.; Dutta, A.; Ramteke, A.; Maji, T. K. Preparation, characterization and cytotoxic applications of curcumin-(±) α-lipoic acid coloaded phosphorylated chitosan nanoparticles in MDA MB 231 breast cancer cell line. *Polym. Adv. Technol.* **2020**, *31* (11), 2827−2841.

(12) Wang, J.; Tang, J.; Zhou, X.; Xia, Q. Physicochemical characterization, identification and improved photo-stability of alpha-lipoic acid-loaded nanostructured lipid carrier. *Drug development and industrial pharmacy* **2014**, *40* (2), 201−210.

(13) Bao, Y.; Guo, Y.; Zhuang, X.; Li, D.; Cheng, B.; Tan, S.; Zhang, Z. D-α-tocopherol polyethylene glycol succinate-based redox-sensitive paclitaxel prodrug for overcoming multidrug resistance in cancer cells. *Mol. Pharmaceutics* **2014**, *11* (9), 3196−3209.

(14) Cao, N.; Feng, S.-S. Doxorubicin conjugated to d-α-tocopheryl polyethylene glycol 1000 succinate (TPGS): conjugation chemistry, characterization, in vitro and in vivo evaluation. *Biomaterials* **2008**, *29* (28), 3856−3865.

(15) Sheng, S.; Zhang, T.; Li, S.; Wei, J.; Xu, G.; Sun, T.; Chen, Y.; Lu, F.; Li, Y.; Yang, J. Targeting vitamin E TPGS−cantharidin conjugate nanoparticles for colorectal cancer therapy. *RSC Adv.* **2015**, *5* (66), 53846−53856.

(16) Khare, V.; Sakarchi, W. A.; Gupta, P. N.; Curtis, A. D.; Hoskins, C. Synthesis and characterization of TPGS−gemcitabine prodrug micelles for pancreatic cancer therapy. *RSC Adv.* **2016**, *6* (65), 60126−60137.

(17) Tavares Luiz, M.; Delello Di Filippo, L.; Carolina Alves, R.; Sousa Araujo, V. H.; Lobato Duarte, J.; Maldonado Marchetti, J.; Chorilli, M. The use of TPGS in drug delivery systems to overcome biological barriers. *Eur. Polym. J.* **2021**, *142*, 110129.

(18) Kumari, S.; Sharma, P.; Mazumder, A. G.; Rana, A. K.; Sharma, S.; Singh, D. Development and validation of chemical kindling in adult zebrafish: A simple and improved chronic model for screening of antiepileptic agents. *Journal of Neuroscience Methods* **2020**, *346*, 108916.

(19) Najib, N. H.; Nies, Y. H.; Abd Halim, S. A.; Yahaya, M. F.; Das, S.; Lim, W. L.; Teoh, S. L. Modeling Parkinson's Disease in Zebrafish. *CNS & Neurological Disorders-Drug Targets (Formerly Current Drug Targets-CNS & Neurological Disorders)* **2020**, *19* (5), 386−399.

(20) Babin, P. J.; Goizet, C.; Raldúa, D. Zebrafish models of human motor neuron diseases: advantages and limitations. *Progress in neurobiology* **2014**, *118*, 36−58.

(21) Lu, C.; Kim, B. M.; Lee, D.; Lee, M. H.; Kim, J. H.; Pyo, H.-B.; Chai, K. Y. Synthesis of lipoic acid−peptide conjugates and their effect on collagen and melanogenesis. *European journal of medicinal chemistry* **2013**, *69*, 449−454.

(22) Sharma, P.; Kumari, S.; Sharma, J.; Purohit, R.; Singh, D. Hesperidin interacts with CREB-BDNF signaling pathway to suppress pentylenetetrazole-induced convulsions in zebrafish. *Frontiers in pharmacology* **2021**, *11*, 2178.

(23) Mazumder, A. G.; Kumari, S.; Singh, D. Anticonvulsant action of a selective phosphatidylinositol-3-kinase inhibitor LY294002 in pentylenetetrazole-mediated convulsions in zebrafish. *Epilepsy research* **2019**, *157*, 106207.

(24) Sharma, S.; Rana, A. K.; Sharma, A.; Singh, D. Inhibition of Mammalian Target of Rapamycin Attenuates Recurrent Seizures Associated Cardiac Damage in a Zebrafish Kindling Model of Chronic Epilepsy. *Journal of Neuroimmune Pharmacology* **2021**, in press. DOI: 10.1007/s11481-021-10021-8

(25) Rana, A. K.; Sharma, S.; Saini, S. K.; Singh, D. Rutin protects hemorrhagic stroke development via supressing oxidative stress and inflammatory events in a zebrafish model. *Eur. J. Pharmacol.* **2022**, *925*, 174973.

(26) Guo, Y.; Niu, B.; Song, Q.; Zhao, Y.; Bao, Y.; Tan, S.; Si, L.; Zhang, Z. RGD-decorated redox-responsive d-α-tocopherol polyethylene glycol succinate−poly (lactide) nanoparticles for targeted drug delivery. *J. Mater. Chem. B* **2016**, *4* (13), 2338−2350.

(27) Dhaundiyal, A.; Jena, S. K.; Samal, S. K.; Sonvane, B.; Chand, M.; Sangamwar, A. T. Alpha-lipoic acid−stearylamine conjugate-based solid lipid nanoparticles for tamoxifen delivery: formulation, optimization, in-vivo pharmacokinetic and hepatotoxicity study. *J. Pharm. Pharmacol.* **2016**, *68* (12), 1535−1550.

(28) Saneja, A.; Sharma, L.; Dubey, R. D.; Mintoo, M. J.; Singh, A.; Kumar, A.; Sangwan, P. L.; Tasaduq, S. A.; Singh, G.; Mondhe, D. M. Synthesis, characterization and augmented anticancer potential of

https://doi.org/10.1021/acs.jafc.2c01685
J. Agric. Food Chem. XXXX, XXX, XXX−XXX

PEG-betulinic acid conjugate. *Materials Science and Engineering: C* **2017**, *73*, 616−626.
(29) Hsieh, P.-W.; Al-Suwayeh, S. A.; Fang, C.-L.; Lin, C.-F.; Chen, C.-C.; Fang, J.-Y. The co-drug of conjugated hydroquinone and azelaic acid to enhance topical skin targeting and decrease penetration through the skin. *Eur. J. Pharm. Biopharm.* **2012**, *81* (2), 369−378.
(30) Li, D.; Liu, S.; Zhu, J.; Shen, L.; Zhu, H. Folic acid modified TPGS as a novel nano-micelle for delivery of nitidine chloride to improve apoptosis induction in Huh7 human hepatocellular carcinoma. *BMC Pharmacology and Toxicology* **2021**, *22* (1), 1−11.
(31) Ruchika; Sharma, A.; Saneja, A. Zebrafish as a powerful alternative model organism for preclinical investigation of nano-medicines. *Drug Discovery Today* **2022**, *27*, 1513.
(32) Igartúa, D. E.; Azcona, P. L.; Martinez, C. S.; del Valle Alonso, S.; Lassalle, V. L.; Prieto, M. J. Folic acid magnetic nanotheranostics for delivering doxorubicin: toxicological and biocompatibility studies on Zebrafish embryo and larvae. *Toxicology and applied pharmacology* **2018**, *358*, 23−34.
(33) Yi, H.; Zhou, X.; Zhou, C.; Yang, Q.; Jia, N. Liquid exfoliated biocompatible WS 2@ BSA nanosheets with enhanced theranostic capacity. *Biomaterials Science* **2021**, *9* (1), 148−156.
(34) Huang, R.-Q.; Bell-Horner, C. L.; Dibas, M. I.; Covey, D. F.; Drewe, J. A.; Dillon, G. H. Pentylenetetrazole-induced inhibition of recombinant γ-aminobutyric acid type A (GABAA) receptors: mechanism and site of action. *Journal of Pharmacology and Experimental Therapeutics* **2001**, *298* (3), 986−995.
(35) Liu, R.; Wu, S.; Guo, C.; Hu, Z.; Peng, J.; Guo, K.; Zhang, X.; Li, J. Ibuprofen exerts antiepileptic and neuroprotective effects in the rat model of pentylenetetrazol-induced epilepsy via the COX-2/NLRP3/IL-18 pathway. *Neurochem. Res.* **2020**, *45* (10), 2516−2526.
(36) Baraban, S. C.; Taylor, M.; Castro, P.; Baier, H. Pentylenetetrazole induced changes in zebrafish behavior, neural activity and c-fos expression. *Neuroscience* **2005**, *131* (3), 759−768.
(37) Kumari, S.; Mazumder, A. G.; Bhardwaj, A.; Singh, D. Early α-linolenic acid exposure to embryo reduces pentylenetetrazol-induced seizures in zebrafish larva. *Prostaglandins, Leukotrienes and Essential Fatty Acids* **2019**, *143*, 15−20.
(38) Dang, J.; Paudel, Y. N.; Yang, X.; Ren, Q.; Zhang, S.; Ji, X.; Liu, K.; Jin, M. Schaftoside suppresses pentylenetetrazol-induced seizures in zebrafish via suppressing apoptosis, modulating inflammation, and oxidative stress. *ACS chemical neuroscience* **2021**, *12* (13), 2542−2552.
(39) Jin, M.; Zhang, B.; Sun, Y.; Zhang, S.; Li, X.; Sik, A.; Bai, Y.; Zheng, X.; Liu, K. Involvement of peroxisome proliferator-activated receptor γ in anticonvulsant activity of α-asaronol against pentylenetetrazole-induced seizures in zebrafish. *Neuropharmacology* **2020**, *162*, 107760.
(40) Dalle-Donne, I.; Rossi, R.; Giustarini, D.; Milzani, A.; Colombo, R. Protein carbonyl groups as biomarkers of oxidative stress. *Clinica chimica acta* **2003**, *329* (1−2), 23−38.
(41) Zheng, Y.-M.; Chen, B.; Jiang, J.-D.; Zhang, J.-P. Syntaxin 1B mediates berberine's roles in epilepsy-like behavior in a pentylenetetrazole-induced seizure zebrafish model. *Frontiers in Molecular Neuroscience* **2018**, *11*, 378.
(42) Zhang, J.; Zhang, D.; McQuade, J. S.; Behbehani, M.; Tsien, J. Z.; Xu, M. C-fos regulates neuronal excitability and survival. *Nature genetics* **2002**, *30* (4), 416−420.
(43) Alachkar, A.; Azimullah, S.; Lotfy, M.; Adeghate, E.; Ojha, S. K.; Beiram, R.; Łażewska, D.; Kieć-Kononowicz, K.; Sadek, B. Antagonism of histamine H3 receptors alleviates pentylenetetrazole-induced kindling and associated memory deficits by mitigating oxidative stress, central neurotransmitters, and c-fos protein expression in rats. *Molecules* **2020**, *25* (7), 1575.
(44) Siddiqui, M. A.; Akhter, J.; Bashir, D. J.; Manzoor, S.; Rastogi, S.; Arora, I.; Aggarwal, N. B.; Samim, M. Resveratrol loaded nanoparticles attenuate cognitive impairment and inflammatory markers in PTZ-induced kindled mice. *International Immunopharmacology* **2021**, *101*, 108287.

https://doi.org/10.1021/acs.jafc.2c01685
J. Agric. Food Chem. XXXX, XXX, XXX−XXX

Journal of Drug Delivery Science and Technology 81 (2023) 104238

Contents lists available at ScienceDirect

Journal of Drug Delivery Science and Technology

journal homepage: www.elsevier.com/locate/jddst

Research paper

A solid dispersion of *Citrus reticulata* peel biowaste as an effective antiepileptic: Sustainable approach toward value addition and agro-industrial waste valorisation

Pallavi Sharma [a,c], Ruchika [b,c], Poonam Dhiman [a,c], Rajneesh Kumar [a,c], Ankit Saneja [b,c], Damanpreet Singh [a,c,*]

[a] *Pharmacology and Toxicology Laboratory, Dietetics and Nutrition Technology Division, CSIR-Institute of Himalayan Bioresource Technology, Palampur, 176061, Himachal Pradesh, India*

[b] *Formulation Laboratory, Dietetics and Nutrition Technology Division, CSIR-Institute of Himalayan Bioresource Technology, Palampur, 176061, Himachal Pradesh, India*

[c] *Academy of Scientific and Innovative Research (AcSIR), Ghaziabad, 201002, India*

ARTICLE INFO

Keywords:
Citrus
Flavonoids
Seizures
Solid dispersion
Soluplus®

ABSTRACT

Flavonoids are the major compounds found in citrus plants, including peel, which is usually considered a biowaste. Numerous studies have indicated possible beneficial effects of citrus flavonoids in epileptic seizures and associated conditions. However, poor solubility and low bioavailability of flavonoids are the primary impediments to their therapeutic use. Hence, in an effort toward waste utilization and value addition, the present study was carried out to improve the solubility and antiseizure efficacy of the citrus peel bioactive flavonoids by utilizing a solid dispersion approach. Solid dispersion of *Citrus reticulata* ethanolic peel extract was formulated using a fourth-generation copolymer, Soluplus®, as carrier and tested in a zebrafish seizure model. An ethanolic (80%) extract of *Citrus reticulata* peel was spray dried with Soluplus polymer matrix, and the resultant solid dispersion was examined morphologically using a scanning electron microscope. The composition and molecular interactions between flavonoids and carrier matrix were observed by Fourier transform infrared spectroscopy. The results revealed a significantly better efficacy of the developed solid dispersion, indicated by a reduction in hyperactive responses, delay in seizure onset, and downregulation in *cellular oncogene fos* (*c-fos*) mRNA expression in zebrafish larvae subjected to pentylenetetrazol. The *in vitro* dissolution of the major flavonoid of the extract showed a steady increase in dissolution percentage with a burst release of hesperidin in the initial 20 min to around 50% in a simulated intestinal fluid media. The study concluded that solid dispersion is a suitable alternative for enhancing the dissolution profile of the citrus peel flavonoids to increase their therapeutic efficacy.

1. Introduction

Citrus fruits are a rich source of bioactive flavonoids. The fruits are also used as a raw material by certain food industries for the production of jellies, juices, jams, drinks, concentrates, *etc*. Annual global production of the common citrus fruits primarily tangerines, grapefruits, oranges, mandarins, limes and lemons are around 102 million tonnes [1]. The peel waste generated after the use of fruit pulp is largely dumped as a waste, despite its richness in a variety of bioactive metabolites. The peel of citrus fruits comprises a high content of polymethoxylated flavones, whereas the pulp is rich in their methylated equivalents that are pharmacologically less active than the former [2]. Hesperidin, nobiletin, rutin, naringin, and other pharmacologically important flavonoids are present abundantly in citrus peel, which are well known to possess pharmacological effects [3,4]. Recently, a study systematically extracted the peels of industrially important citrus fruits, including *Citrus reticulata* c. v., *Citrus grandis*, *Citrus sinensis*, *Citrus reticulata* Blanco, and *Citrus limetta*. The study found that extraction of the citrus peels with 80% ethanol (v/v) as a solvent yielded a maximum quantity of extract. Among all, *Citrus reticulata* (*C. reticulata*) extract showed a

* Corresponding author. Pharmacology and Toxicology Laboratory, CSIR-Institute of Himalayan Bioresource Technology, Palampur, 176061, Himachal Pradesh, India.

E-mail addresses: damanpreet@ihbt.res.in, dsinghpharmacology@gmail.com (D. Singh).

https://doi.org/10.1016/j.jddst.2023.104238
Received 28 October 2022; Received in revised form 15 January 2023; Accepted 1 February 2023
Available online 10 February 2023
1773-2247/

potent antioxidant efficacy. High-performance liquid chromatography (HPLC)-based quantification showed the highest amount of hesperidin in the *C. reticulata* extract, followed by nobiletin, quercetin, tangeretin, rutin, apigenin and naringin. Further, *in vitro* and *in silico* studies supported the neuroprotective efficacy of the extract due to the presence of flavonoids [5]. Thus, suggesting that peel extracts be an ideal therapeutic agent for the chronic neurological condition.

Epilepsy is a chronic neurological condition, marked by a persistent predisposition to generate seizures. Epilepsy affects both sexes and people of all ages, with an estimated global prevalence of around 65 to 70 million people [6]. The International League Against Epilepsy defines it as at least two unprovoked seizures that happen more than 24 h apart [7]. There is a diverse range of antiepileptic drugs available in the market today. However, efficacy, tolerability, adverse drug reactions, and tendency to generate or aggravate seizures related comorbidities are the key concerns related to the currently available drug therapy. Given the complicated mechanisms involved in epileptogenesis and underlying comorbid conditions, innovative and more effective therapeutic approaches are of greatest need. In this regard natural-products based therapies have been suggested as a potential agent for epilepsy management [8]. Furthermore, several studies have suggested that neuroprotective flavonoids suppress epileptic seizures via multiple mechanisms [9,10]. Hence, all these findings suggested a possible antiepileptic potential of citrus peel extracts with proven neuroprotective efficacy.

The beneficial effects of dietary flavonoids on mental health and neurophysiological disorders have gained a lot of interest in the recent decades. The neuroprotective properties of citrus flavonoids and their molecular targets have been investigated in a number of studies [4,9]. Despite the therapeutic claims made about flavonoids, it is well accepted that their poor solubility, membrane permeability, and stability profile limit their oral bioavailability and thus therapeutic efficacy. After being consumed orally, flavonoids are absorbed through the intestine. The amount of flavonoid that makes it to the systemic circulation is decided by cell membrane penetrability, presystemic metabolism and protein binding [11,12]. All these characteristics are assumed to be regulated by flavonoid's chemical structure. In general, the small intestine absorbs up to 60% of the total flavonoids consumed, with an elimination half-life ranging from 2 to 28 h [13]. Therefore, techniques that can enhance the bioavailability of flavonoids are of great interest to the researchers. According to some recent studies, solid dispersion formulated by utilizing a variety of processes and carriers is an excellent method for enhancing solubility of flavonoids [14]. Soluplus® (SOL) is a fascinating polymer which can be used as a carrier for solid dispersion formulations. It is a tri-block polymeric solubilizer made up of monomeric polyvinyl caprolactam-polyvinyl acetate-polyethylene glycol subunits. Its solubility does not change throughout the gastrointestinal tract due to its amphiphilic and non-ionic properties. Furthermore, it has a minor surface-active property that aids in the maintenance of super saturation state of poorly soluble molecules [15].

Therefore, in an attempt toward value-addition of citrus peel for therapeutic use, the present study focused on the development of a solid dispersion of *C. reticulata*. It is the most popular mandarin grown worldwide, with a variety of names, excellent eating quality, and high polyphenol content. Worldwide, the industrial processing of *C. reticulata* generates millions of tonnes of organic waste [16]. In the study, the spray drying technique was used for the encapsulation of peel extract of *C. reticulata* in the SOL polymer matrix. However, to our best knowledge, this is the first effort to deliver citrus peel extract with SOL for a neurological condition. The antiseizure efficacy of the developed solid dispersion was tested in 7-day-old Zebrafish (*Danio rerio*) larvae using the pentylenetetrazole (PTZ)-induced convulsion model. In drug delivery studies, the use of zebrafish is now being encouraged due to its multiple benefits over rodent models [17]. It has emerged as an ideal model for neurological conditions as its central nervous system exhibits a lot of anatomical, functional, molecular, and genetic resemblance with vertebrates [18]. In earlier experiments, zebrafish have also been utilized to study the efficacy of a solid lipid nanoparticles of a flavonoid in epilepsy [19].

2. Material and methods

2.1. Drugs and chemicals

PTZ and Trizol reagent was acquired from Sigma Aldrich, USA. GoTaq qPCR Master Mix was obtained from Promega, United States. Verso cDNA synthesis kit was procured from Thermo Fisher Scientific, USA. Sea salt was obtained from Aquarium Systems, Germany. Sodium dodecyl sulfate (Lot number MKBX0092V) was purchased from Sigma Aldrich, USA. SOL (Lot No. 20747936W0) was received as a gift sample from the BASF India Limited, Navi Mumbai, India. All of the solvents used were of the analytical grade.

2.2. Animals and ethics

Wild-type zebrafish were kept in a conventional stand-alone system aquatic environment (Tecniplast, Buguggiate, Varese, Italy). The fish water from the circulating system supplied constant aeration. The pH, conductivity, and temperature of the fish water were maintained at 7.0 to 7.5, 400 to 600 μS and 26–28 °C, respectively. The fish were fed live artemia twice a day (Inve Aquaculture, Inc., Salt LakeCity, USA). Fish were exposed to a light and dark cycle of 14:10 h. Healthy embryos were collected after breeding of fish, as described earlier [20]. Embryos were then cleaned followed by incubation in biological oxygen demand incubator (Relitech, Ambala, India) till 7 *dpf* (days post fertilization) with regular change of water. The study protocol was approved by the Institutional Animal Ethics Committee (IAEC) of CSIR-IHBT established under Committee for the Purpose of Control and Supervision of Experiments on Animals, Ministry of Fisheries Animal Husbandry and Dairying, Department of Animal Husbandry and Dairying, Government of India (Approval Number: IAEC/IHBT P-2/April2021; dated 23rd April 2021).

2.3. Extraction and HPLC-based quantification

C. reticulata peel collection, processing, extraction, and quantification was done as described earlier [21]. The peel collection was done between the months of November to January, which is the prime harvesting time of citrus fruits. It was then identified by a food technologist. The collected peel was dried in hot air oven at 40 °C, chopped into small pieces, ground using a mixer grinder (Philips, India) and sieved (mesh size of 500 μm). The extraction process involved an initial 20 min thermal treatment (80 °C) of the powdered material with solvent (1:10 w/v), followed by overnight maceration at room temperature. The collected extract was filtered, concentrated using Rotavapor® R-300 (Buchi), and finally lyophilized using Labconco FreeZone 6 Plus Lyophilizer. The process involved initial freezing of the concentrated sample at −20 °C, and finally lyophilisation −55 °C under vacuum until dried (48 h). The extract was thereafter subjected to HPLC-based quantification of a major flavonoid.

As in our earlier finding [5], we observed *C. reticulata* peel extract to contain the highest amount of hesperidin, and the flavonoid also showed a potent anticonvulsant effect in a previous experiment [22]. Hence, hesperidin was quantified as a major biomarker for the extract quantification, and further release study. The quantification was carried out on a Shimadzu HPLC system, coupled with a photodiode array (PDA) detector. A previously reported method was used for the quantification of hesperidin [23]. The chromatographic separation was performed on a RP-18 column (250 × 4.6 mm; 5 μm, Waters) with a gradient mobile phase combination of water (0.1% formic acid) and acetonitrile (0.05% formic acid) was used as the mobile phase. The flow rate was set to 1 mL/min and the column temperature was set to 30 °C. The

quantification was carried out in triplicate.

2.4. Solid dispersion development using spray drying method

Solid dispersion of *C. reticulata* extract was formulated by using SOL as solid carrier via spray drying method. Briefly, amorphous solid dispersion of citrus extract with SOL was developed by blending the SOL (1% w/v solution) and extract 2:1 (w/w) ratio in binary solvent system of water and ethanol (1:1). The resultant solution was fed to Buchi Mini Spray Dryer B-290 with 75% aspirator, 14% pump and 120 °C inlet temperature settings. The prepared solid dispersion (*extSD*) was stored in desiccator until further analysis. The encapsulation efficiency was determined by a standard method of HPLC and calculated as follows:

$$\textit{Encapsulation efficiency}\ (\%) = \frac{\textit{Amount of hesperidin in extSD}}{\textit{Initial amount of hesperidin in extract}} \text{X } 100$$

2.5. Particle size analysis and scanning electron microscopy studies

The particle size and polydispersity index of the *extSD* were measured by dynamic light scattering (Malvern Zetasizer Nano ZS90, Malvern Instruments Ltd. Malvern, UK) at 25 °C. Prior to analysis, the spray-dried *extSD* was dispersed in Milli-Q water. The surface morphology of SOL, PM (physical mixture of SOL and *C. reticulata* extract in the ratio of 2:1) and *extSD* was studied by using Scanning electron microscope (S–3400 N Hitachi, Japan) with acceleration voltage of 15 kV. Briefly, each sample was fixed on metal stub using double side adhesive carbon tape and covered with a thin gold film using Hitachi Ion Sputter (E−1030). The samples were exposed to the Au for 2.5 min and thereafter examined under the scanning electron microscope.

2.6. Fourier transform infrared spectroscopy (FTIR) analysis

FTIR spectra of the SOL, *C. reticulata* extract, PM, and *extSD* were obtained by using PerkinElmer FTIR spectrophotometer (PerkinElmer, Waltham, USA). Analysis of all samples was performed by potassium bromide disk method. The samples were dispersed in dry potassium bromide and the disk was placed in the FTIR sample holder in absorbance mode. FTIR spectra were recorded in the form of percent transmittance over a spectral range from 4000 to 500 cm^{-1} wavenumber with a resolution of 1 cm^{-1} [24].

2.7. In vitro dissolution studies

In vitro dissolution studies of the extract and *extSD* were carried out using USP II dissolution apparatus (LABINDIA analytical, Mumbai, India; Type 2: Paddle) under sinking conditions [25]. Briefly, the samples with known concentration of hesperidin (marker flavonoid) were filled in hard gelatine capsules and dropped into the dissolution media (simulated intestinal fluid pH 6.8 with 0.25% sodium lauryl sulfate, 900 mL) with mild stirring conditions of 100 rpm. The bowl temperature was maintained at 37 ± 0.5 °C and aliquots of 5 mL were collected at the fixed time intervals (0, 5, 15, 30, 45, 60, 90 and 120 min) with immediate replenishing of the media by adding equal volume of withdrawn amount [26]. The samples were filtered and analysed by HPLC for the hesperidin quantification using the earlier mentioned method (see section extraction and HPLC-based quantification). All samples were analysed in triplicate.

2.8. PTZ-induced seizures in larva

The experiment was carried out in a transparent 6-well flat-bottomed plate with individual wells measuring 3.5 cm (diameter), as described earlier [27]. At 7 *dpf*, the zebrafish larvae were divided into 4 groups (n = 6), and initially incubated with *C. reticulata* extract concentrations of 25 μg/mL, 50 μg/mL, 100 μg/mL, and *extSD* 100 μg/mL (uniformly dissolved in fish water) represented as *ext25/ptz*, *ext50/ptz*, *ext100/ptz*, and *extSD100/ptz,* respectively for 1 h. Additionally, 2 separate groups of larvae were used as naive (*sw/sw*) and vehicle (*sw/ptz*) control, and were initially incubated in the fish water. The larvae of the *ext25/ptz*, *ext50/ptz*, *ext100/ptz*, *extSD100/ptz*, and *sw/ptz* groups were placed individually in wells filled with PTZ (8 mM) after the initial incubation. The PTZ exposure to larvae results in appearance of hyperactivity (increased irregular swimming activity; Stage 1), circular movements (whirlpool-like motion; Stage 2) and clonus-like seizures with single-sided or total loss of posture (Stage 3) [28]. The hyperactive responses in all the groups were recorded for the initial 5 min as a measure of the total distance traveled and mean velocity with a camera (c922 Pro Stream, Logitech, Hong Kong) connected to a video tracking system (SMART V.3.0, Panlab Barcelona). The *sw/sw* group recordings were made in the fish water. Further, the latency to the first clonus-like seizure (stage 3) was also noted in the group subjected to PTZ with an upper cut off time of 15 min. The solution was kept at 28 ± 1 °C and was changed after each recording.

2.9. Gene expression studies

The larvae at 7 *dpf* were divided into 3 different groups as *sw/ptz-s*, *ext100/ptz-s* and *extSD100/ptz-s*, and were incubated in the fish water, 100 μg/mL of *C. reticulata* extract (highest effective concentration) and 100 μg/mL of *extSD*, respectively for 1 h. Each group contained 3 independent sets (n = 20/set). After the incubation, 15 min exposure of PTZ (8 mM) was given to all the groups. Additionally, a separate naïve group (*sw/sw-s*) with 3 independent sets of larvae (n = 20/set) was placed in the fish water without PTZ. After the respective exposures, all the larvae were sacrificed by cryoanesthesia and the whole head was isolated. After that the Trizol reagent (Sigma Aldrich, USA) method was used for extraction of total RNA from the larvae head. The tissue was homogenized with Trizol reagent, chloroform was added and incubated for 5 min at room temperature, followed by centrifugation at 12,000 g at 4 °C (SL8R Thermo Fisher Scientific, USA) for 15 min. The aqueous supernatant layer was taken out in a separate tube and isopropanol was added to precipitate RNA followed by centrifugation. The obtained RNA pellet was washed with 75% ethanol followed by centrifugation. RNA pellet was dissolved in nuclease free water followed by quantification using a Nanodrop (ND-1000 Thermo Scientific, USA). RNA was reverse transcribed into cDNA with the help of Verso cDNA synthesis kit (Thermo Fisher Scientific, USA). The quantitative real-time polymerase chain reaction (qRT-PCR) analysis was accomplished using GoTaq qPCR Master Mix (Promega, USA) on AriaMx Real-Time PCR System (Agilent Technologies, USA) [29]. Each analysis was performed in triplicate and the mean values was considered. Primer3 Input (v.0.4.0) software was used for primer design. The quantification of *cellular oncogene fos* (*c-fos*) was performed with *eef1a1b* (eukaryotic translation elongation factor 1alpha 1b) as internal standard. The primer sequences of *c-fos* and *eef1a1b* were [F: TTACCGGTGCTAGATTTGTT; R: ATTCACACGTTCAGAAATCC], and [F: TATCTCAAAGAACGGGCAAA; R: TTCACAATCTCCTCATAGCG], respectively. 2ˆddCT method was used for gene expression analysis and the values expressed as fold change with respect to *sw/sw-s*.

2.10. Statistical analysis

The results of latency to first clonic-like seizure, distance traveled, and average speed were shown as mean ± standard error of the mean. Whereas the results of hesperidin quantification, gene expression analysis and *in vitro* dissolution studies were presented as mean ± standard deviation. The statistical analysis was performed using one-way analysis of variance followed by Tukey's *post hoc* test. The results with $P < 0.05$ were considered as significant. The SigmaStat® software was used for statistical analysis.

3. Results

3.1. Extraction and quantification of flavonoids

The thermally assisted maceration of *C. reticulata* peel powder with 80% ethanol yielded 21.88% w/w of the dried extract. Further, the HPLC-PDA based quantification showed hesperidin content to the extent of 559.61 ± 53.27 μg/100 mg of the crude extract (Fig. 1). The extract yield from the peel powder, and hesperidin content was in line with the previous study [21].

3.2. Solid dispersion optimization

The *extSD* of extract was formulated to enhance the solubility and the therapeutic efficacy of polyphenolic compounds present in the extract. The resultant *extSD* of plant extract (ratio 2:1) was finalized on the basis of encapsulation and loading efficiency. The finalized formulation, *extSD* obtained was slightly orange coloured (due to the extract colour) powder. The encapsulation efficiency of the optimized formulation was found to be 92%.

3.3. Particle size and surface morphology studies

The scanning electron microscopy images of SOL, PM, and *extSD* were captured to study the sample's surface morphology and shape. The image of SOL revealed their large size with uneven and irregular surface (Fig. 2A). Whereas, SEM image of *extSD* powder indicated micro particles with smooth surface. Moreover, a substantial difference in the morphology of PM (Fig. 2B) and *extSD* (Fig. 2C) was observed. The images of *extSD* also represented a successful encapsulation of extract and homogenous distribution of the extract in the solid dispersion [30]. After dispersion of *extSD* in Milli-Q water, the *extSD* self-assembled into micelles with the average particle size of about 78.41 ± 2.40 nm with a polydispersity index of 0.070 ± 0.008 (Fig. 2 D) which is in line with the previously published reports on SOL [31,32].

3.4. Molecular interaction analysis

The FTIR spectra of SOL, *C. reticulata* extract, PM and *extSD* was recorded to determine the possible molecular interactions between extract components and the wall material. The spectra of SOL exhibited characteristic peaks at 3549.47 cm^{-1}, 3471.99 cm^{-1}, 3418.59 cm^{-1}, 2930.83 cm^{-1}, 2858.76 cm^{-1} and 1618.27 cm^{-1} of hydroxyl, aliphatic acid carbonyl region [33]. The broad peaks at 3369.79 cm^{-1} region in the extract may be due to the presence of various hydroxyl groups of the compounds present in it. No spectral shift was found in the spectra of PM of SOL and extract, indicating no interactions (Fig. 3 A). Moreover, in *extSD* broadening of peak at 3400 cm^{-1} region in comparison to extract may be due to possible hydrogen bonding interaction between both the components, corresponding to the previous findings reported earlier showing characteristic broad absorption stretching vibrations of hydrogen bond at around 3400 cm^{-1} [34].

3.5. In vitro dissolution analysis

Solid dispersions are known to enhance the solubility. Hence, *in vitro* dissolution test was performed to determine the dissolution profile of the *extSD* with hesperidin as a marker. Fig. 3B illustrates the *in vitro* dissolution profile of hesperidin for *extSD* in simulated intestinal fluid (pH 6.8) with 0.25% sodium lauryl sulfate as dissolution media. The data demonstrated that *extSD* showed a steady increase in the dissolution percent with a burst release of hesperidin in the initial 20 min to approximately 50%. The substantial increase in the dissolution of marker molecule of extract observed was due to the decrease in particle size, increase in surface area and surrounding of hydrophilic carrier [33, 35,36]. However, the percent release of hesperidin in the crude extract remained below the limit of detection. Hence, not included in the figure.

3.6. Effect of solid dispersion on PTZ-mediated hyperactive responses

PTZ exposure in *sw/ptz* group initially showed an abnormal increase in the swimming activity. There was a significant ($P < 0.001$) increase in the total distance traveled in *sw/ptz* group compared to *sw/sw* group. *C. reticulata* extract treatment resulted in a significant dose-dependent decrease in the total distance traveled in *ext25/ptz* ($P = 0.011$), *ext50/ptz* ($P = 0.005$) and *ext100/ptz* ($P < 0.001$) groups compared to *sw/ptz* group. A statistically ($P < 0.001$) similar decrease in the distance moved by the larvae was observed in *extSD100/ptz* group treated with the developed *extSD* compared to *sw/ptz* group, as that of highest extract concentration. However, no change in the total distance traveled was observed among the extract and the formulation-treated groups (Fig. 4A). Similar observations were observed on the mean swimming speed. PTZ resulted in a significant ($P < 0.001$) increase in the swimming speed in *sw/ptz* group compared to the naïve *sw/sw* group. A dose-dependent decrease in the speed was observed following incubation with 25 μg/mL ($P = 0.01$), 50 μg/mL ($P = 0.006$), 100 μg/mL ($P < 0.001$) of the *C. reticulata* extract compared to *sw/ptz* group. The *extSD* showed a similar reduction ($P < 0.001$) in the swimming speed compared to *sw/ptz* group as that of *ext100/ptz* group (Fig. 4B).

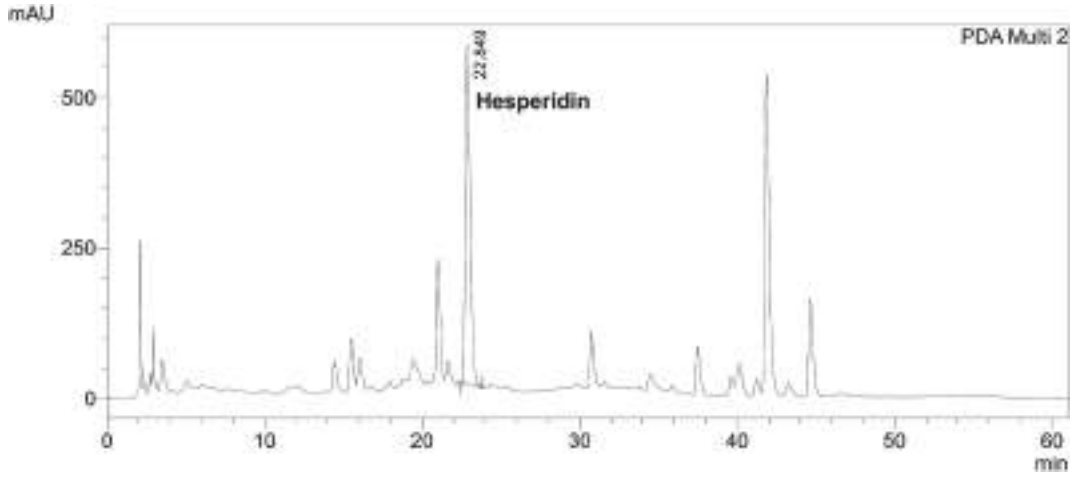

Fig. 1. The HPLC-PDA chromatogram of *C. reticulata* peel extract with hesperidin peak.

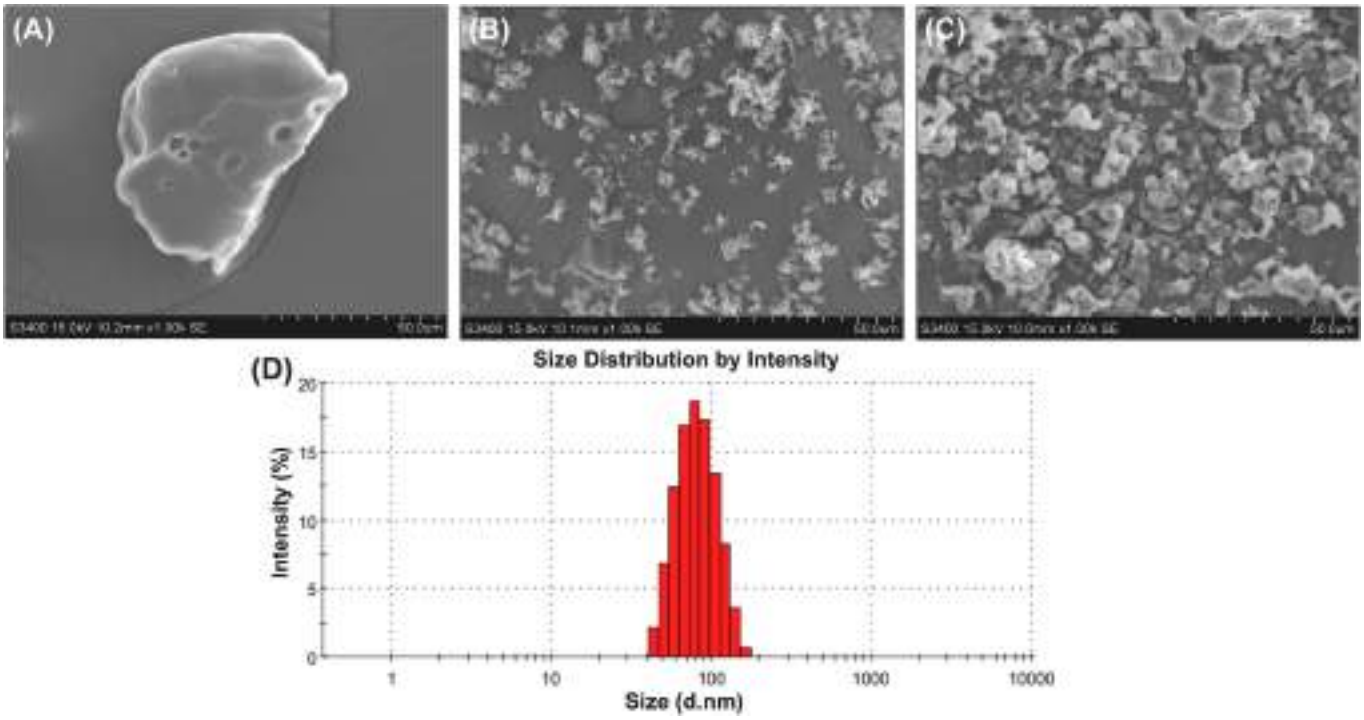

Fig. 2. Scanning electron microscopy images of SOL **(A)**, PM **(B)** *extSD* **(C)**. The particle size distribution of *extSD* shown in figure **(D)**.

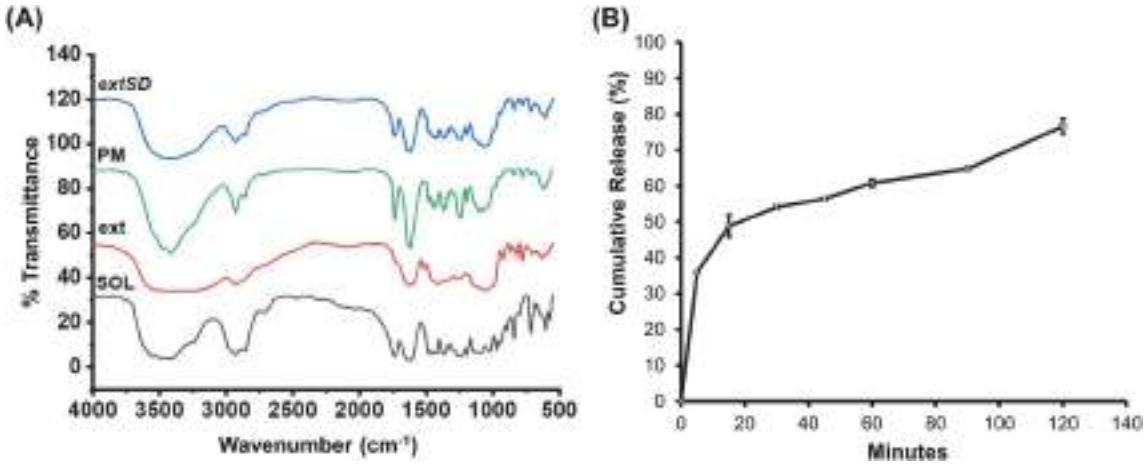

Fig. 3. FTIR spectra of SOL, *C. reticulata* peel extract (ext), physical mixture (PM), and the developed Solid dispersion (*extSD*) (**A**) and; *In vitro* cumulative release (%) of hesperidin from the developed solid dispersion in simulated intestinal fluid (**B**).

3.7. Effect of solid dispersion on PTZ-mediated clonic-like seizures

The extract at 25 μg/mL and 50 μg/mL showed insignificant change in latency to first PTZ-mediated clonic-like seizure in *ext25/ptz* ($P = 1.00$) and *ext50/ptz* ($P = 0.939$) groups respectively, compared to *sw/ptz* group. The *C. reticulata* extract at 100 μg/mL significantly increased the seizure latency as compared to *sw/ptz* ($P = 0.007$), *ext25/ptz* ($P = 0.007$) and *ext50/ptz* groups ($P = 0.039$). The developed *extSD* treatment in *extSD100/ptz* group showed a significant delay in the appearance of clonic-like seizures compared to *sw/ptz* ($P < 0.001$), *ext25/ptz* ($P < 0.001$), *ext50/ptz* ($P < 0.001$) and *ext100/ptz* groups ($P = 0.005$). The results showed *extSD* to be more efficacious in seizure suppression compared to the extract (Fig. 5A).

3.8. Effect on the brain c-fos expression

PTZ-mediated seizures resulted in a significant ($P < 0.001$) increase in the expression of *c-fos* in the larvae brain of *sw/ptz-s* compared to *sw/sw-s*. The extract treatment at 100 μg/mL concentration resulted in a marked ($P < 0.001$) reduction in the *c-fos* expression of *ext100/ptz-s* group compared to *sw/ptz-s* group. The developed *extSD* showed maximum protection as its treatment resulted in a significant ($P < 0.001$) reduction in the brain *c-fos* expression in *extSD100/ptz-s* group compared to *ext100/ptz-s* and *sw/ptz-s* groups. However, the expression remained significantly higher in *extSD100/ptz-s* and *ext100/ptz-s* groups compared to the naïve *sw/sw-s* group (Fig. 5B).

4. Discussion

The present study showed that the solid dispersion prepared from an

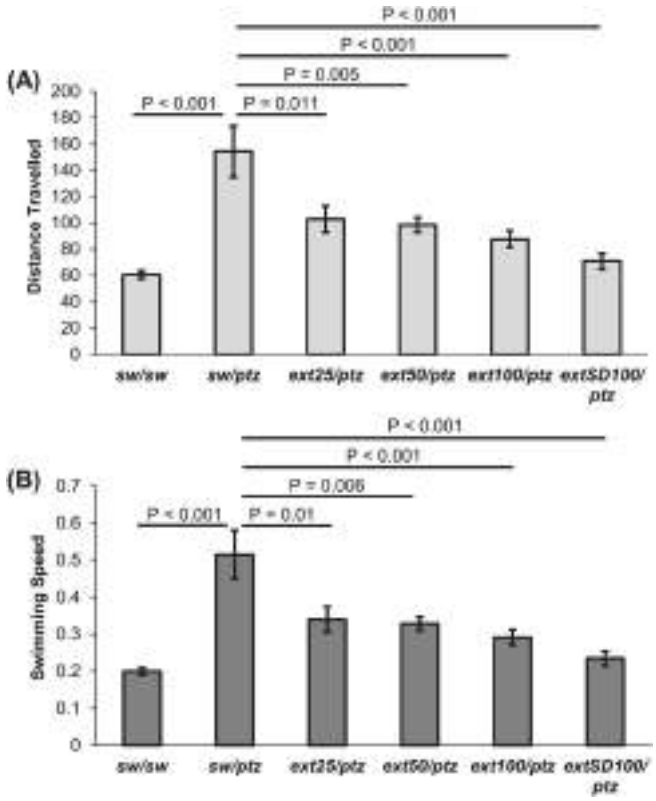

Fig. 4. Effect of *C. reticulata* peel extract and the developed solid dispersion on PTZ-mediated hyperactive response of zebrafish larvae shown as total distance traveled in cm (A) and mean speed in cm/s (B). *sw/sw*: Group of larvae incubated with fish water and not exposed to PTZ; *sw/ptz*: Group of larvae incubated with fish water and exposed to PTZ; *ext25/ptz*: Group of larvae incubated with 25 μg/mL of *C. reticulata* extract and exposed to PTZ; *ext50/ptz*: Group of larvae incubated with 50 μg/mL of *C. reticulata* extract and exposed to PTZ; *ext100/ptz*: Group of larvae incubated with 100 μg/mL of *C. reticulata* extract and exposed to PTZ and; *extSD100/ptz*: Group of larvae incubated with 100 μg/mL of *extSD* and exposed to PTZ.

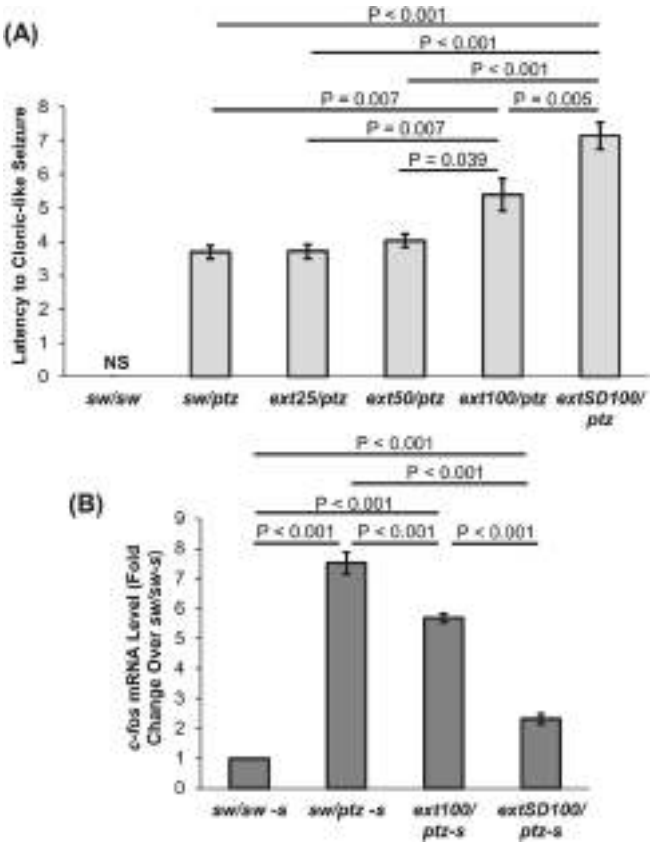

Fig. 5. Effect of *C. reticulata* peel extract and the developed solid dispersion on latency to first PTZ-mediated clonic-like seizure in minutes (A) and the brain *c-fos* expression (B). *sw/sw*: Group of larvae incubated with fish water and not exposed to PTZ; *sw/ptz*: Group of larvae incubated with fish water and exposed to PTZ; *ext25/ptz*: Group of larvae incubated with 25 μg/mL of *C. reticulata* extract and exposed to PTZ; *ext50/ptz*: Group of larvae incubated with 50 μg/mL of *C. reticulata* extract and exposed to PTZ; *ext100/ptz*: Group of larvae incubated with 100 μg/mL of *C. reticulata* extract and exposed to PTZ; *extSD100/ptz*: Group of larvae incubated with 100 μg/mL of *extSD* and exposed to PTZ; *sw/sw-s*: Group of 3 independent sets of larvae incubated with fish water and not exposed to PTZ; *sw/ptz-s*: Group of 3 independent sets of larvae incubated with fish water and exposed to PTZ; *ext100/ptz-s*: Group of 3 independent sets of larvae incubated with 100 μg/mL of *C. reticulata* extract and exposed to PTZ and; *extSD100/ptz-s*: Group of 3 independent sets of larvae incubated with 100 μg/mL of *extSD* and exposed to PTZ. NS: No seizures as not subjected to PTZ.

extract of *C. reticulata* peel and SOL increased the release profile of its major flavonoid and showed an antiepileptic effect in a zebrafish larva model. The *extSD* showed an increased dissolution rate and better antiseizure effect, indicated by increased clonic-like seizure latency and decreased c-fos expression compared to the crude *C. reticulata* extract.

An interest in obtaining bioactive compounds from food waste, such as citrus by-products, using environment-friendly technologies has grown over the past few years. Due to its high-quality fiber, pectin content, and presence of bioactive compounds like polyphenols (flavonoids and phenolic acids), carotenoids, and essential oils, citrus waste is a potential source of compounds with great biological value [37]. However, the low dissolution rate and poor bioavailability of flavonoids limit their application as therapeutic agents. A tight molecular arrangement due to the double bond between positions 2 and 3 of flavones and flavanols makes it difficult for the solvent molecule to pass through. Flavonoids with high molecular weights and complex structures may also have lower bioavailability [11]. Some previous studies have also tested the therapeutic efficacy of citrus fruit waste-derived waste products. In an earlier study performed in our lab, the effectiveness of 80% ethanolic extract of *C. reticulata* peel was tested in a chronic kindling mouse model of epilepsy. The results confirmed an antiseizure potential of the extract in PTZ-kindled mice. However, a significant antiseizure effect was observed after 15 days of repeated extract treatment [21]. The delayed effect could be correlated with the low bioavailability of the pharmacologically active flavonoids present in the extract [5]. Alternative approaches for increasing the bioavailability of these molecules are thus becoming increasingly important. Developing solid dispersions of poorly water-soluble molecules with water-soluble carriers helps to overcome the limitation to a large extent.

The method for preparing the solid dispersion must be cost-effective, environment friendly, and avoid thermal degradation of the drug [38]. The spray drying method was chosen for solid dispersion development in the current study. It is a multi-step process that necessitates the control of variables such as temperature, spray rate, atomization rate, and inlet and outlet air temperature. These variables determine the particle size, particle size distribution, surface properties, and the release of the material [39]. SOL was the carrier of choice, as it has proved to be a promising carrier for poorly water-soluble drugs. It is suitable for the long-term administration of hydrophobic drugs due to its amphiphilicity, low hygroscopicity, and low toxicity. Nowadays, it has been used in a variety of pharmaceutical technologies, including the generation of micelles, solid dispersions, nanoparticles, and self-emulsifying drug delivery systems [40].

Scanning electron microscopy was used to examine the change in particle size and surface morphology of the prepared solid dispersions.

In vivo efficacy of the solid dispersion relies heavily on dissolution studies. Generally, the formulation with the most homogeneity and the highest amorphous drug content has the best dissolution profile. The solid dispersion technique is usually employed to enhance hydrophobic phytochemicals' solubility and dissolution index. Solid dispersions are known to enhance the solubility of encapsulating drugs by changing their crystalline nature into amorphous [41]. In the current study, enhanced solubility and improved dissolution profile of hesperidin was observed after preparation of the solid dispersion. This can be explained by effective molecular dispersion of the *Citrus reticulata* extract in the amphiphilic SOL carrier matrix.

It has been observed that bioactive agents show variation in therapeutic response in acute and chronic seizure models [42]. As mentioned, in the previous study, the antiseizure efficacy of the *C. reticulata* extract was tested in a chronic kindling mouse model that showed a delayed response [21]. Hence, to understand the variation the efficacy of the extract and the developed formulation was tested in an acute seizure model in the present study. Zebrafish larva shows mature swimming behaviour at around 4–5 *dpf* after developing a swim bladder [43]. PTZ, a classical inhibitor of the $GABA_A$ receptor, induces hyperactivity in zebrafish larvae that can be recorded as distance traveled and swimming speed. Anti-hyperactive effect of citrus extract and *extSD* can be credited to the ability of citrus flavonoids to act on GABA receptors. Hesperidin, the major component of citrus peel, has shown an antiseizure effect on zebrafish larvae in an earlier study performed in our lab [22]. The developed *extSD* showed statistically better suppression of PTZ-mediated seizures as well as hyperactive responses. This indicated that formulation of solid dispersion might have resulted in efficient and quick absorption of flavonoids present in the extract due to increased dissolution rate. However, in case of the crude extract the effect was lower due to limited dissolution. Enhanced antiseizure effect in zebrafish larvae can be attributed to the faster release of pharmacologically active flavonoids into the aqueous media from solid dispersion compared with pure extract.

PTZ exposure to zebrafish larvae has been reported to induce seizure-like behaviour. Its exposure results in a series of events, which typically begin with hyperactivity and circular movements, then progress to tonic-clonic-like seizures and loss of posture [28]. In the current study, the latency to the onset of clonic-like seizures in the treated groups was compared with the control as an index of antiseizure effect. Treatment of *extSD* significantly delayed the onset of seizures compared to all of the extract doses tested. The solubility and dissolution-enhancing effects of SOL can be considered the reason behind the enhanced efficacy of the developed *extSD*. In previous studies, formulations made from SOL have also been shown to improve blood-brain barrier penetration. This can result in rapid and enhanced pharmacological effect of the centrally acting compounds [44]. Fleming et al. [45] found that the blood-brain barrier matures in zebrafish larvae between 3 and 10 *dpf* and resembles the mammalian blood-brain barrier to a large extent. Thus, the use of 7 *dpf* zebrafish larvae may provide a rapid and effective model in determining the blood-brain barrier penetrability of novel formulations.

The expression of *c-fos* is observed in various brain regions as early as 15 min after PTZ exposure in zebrafish. *c-fos* is thought to be a good indicator of seizure generation and propagation [46]. According to Labinar et al. [47], seizure-induced *c-fos* expression is linked to continuous neuronal depolarization, increased intracellular calcium and N-methyl-D-aspartate receptor expression. The group treated with the solid dispersion displayed a significant drop in the *c-fos* expression compared to the group treated with a similar concentration of the extract signifying reduced neuronal firing.

Spray drying technique was used to successfully prepare a solid dispersion of *C. reticulata* extract in a SOL carrier matrix, which was then confirmed by SEM and FTIR analysis. The solid dispersion was found to have a stronger antiseizure effect than the crude extract, as evidenced by increased latency to clonic seizures, decreased hyperactive activity, and reduced *c-fos* expression in PTZ-treated zebrafish larvae. The improved solubility profile of solid dispersion can be the reason behind its improved pharmacological action. Formulation of solid dispersion using SOL thus can be considered as potential strategy for improving therapeutic efficacy of the citrus flavonoids.

5. Conclusion

The application of SOL for the formation of *extSD* brought about a considerable improvement in both the dissolution rate and antiseizure efficacy of *C. reticulata* peel extract. Based on the data obtained in the zebrafish model, it can be concluded that the production of amorphous solid dispersion is a cost-effective, sustainable approach with high potential for therapeutic and industrial application toward value addition and waste valorisation.

Author statement

Nil.

Declaration of competing interest

The authors declare that they have no known competing financial interests or personal relationships that could have appeared to influence the work reported in this paper.

Data availability

Data will be made available on request.

Acknowledgement

The authors are thankful to the Director, CSIR-IHBT, Palampur (HP), India, for providing the essential facilities. The authors are also thankful to the BASF India Limited, Navi Mumbai, India for providing SOL as a gift sample. Ms. Pallavi Sharma is grateful to the ICMR, New Delhi, India for granting Senior Research Fellowship (File no: 5/3/8/38/ITR-F/2018-ITR). Ms Ruchika, Ms. Poonam Dhiman and Mr. Rajneesh Kumar are thankful to the CSIR, New Delhi, India for providing Junior Research Fellowship (31/054(0163)/2020-EMR-I), (31/054(0158)/2020-EMR-I), (31/054(0157)2020-EMR-I, respectively). The authors are thankful to the Central Instrumentation Facility at the CSIR- Indian Institute of Integrative Medicine (IIIM), Jammu for conducting FTIR analysis. The authors remain indebted to Mr. Nabab Khan [CSIR JRF-GATE Fellow; File No.: GATE31/0054 (12027)/2021-EMR-I] for providing help in particle size distribution studies. The authors are also thankful to the CSIR, New Delhi, India, for providing financial assistance for the work through MLP-0204 project. The institute's communication number of the manuscript is 5143.

References

[1] J.G. Perez-Perez, I.P. Castillo, A. Garcia-Lidon, P. Botia, F. Garcia-Sanchez, Fino lemon clones compared with the lemon varieties Eureka and Lisbon on two rootstocks in Murcia (Spain), Sci. Hortic. 106 (2005) 530–538.
[2] B. Singh, J.P. Singh, A. Kaur, N. Singh, Phenolic composition, antioxidant potential and health benefits of citrus peel, Food Res. Int. 132 (2020), 109114.
[3] E. Tripoli, M. La Guardia, S. Giammanco, D. Di Majo, M. Giammanco, Citrus flavonoids: molecular structure, biological activity and nutritional properties: a review, Food Chem. 104 (2007) 466–479.
[4] S.L. Hwang, P.H. Shih, G.C. Yen, Neuroprotective effects of citrus flavonoids, J. Agric. Food Chem. 60 (2012) 877–885.
[5] P. Sharma, V. Dadwal, S.N. Rahmatkar, M. Gupta, D. Singh, Flavonoid composition and antioxidant efficacy of citrus peels: an integrated *in vitro* and *in silico* approach toward potential neuroprotective agents, J. Sci. Ind. Res. 81 (2022) 445–454.
[6] E. Beghi, The epidemiology of epilepsy, Neuroepidemiology 54 (2020) 185–191.
[7] A. Singh, S. Trevick, The epidemiology of global epilepsy, Neurol. Clin. 34 (2016) 837–847.
[8] D. Ekstein, S.C. Schachter, Natural products in epilepsy-the present situation and perspectives for the future, Pharmaceuticals 3 (2010) 1426–1445.

[9] P. Sharma, A. Kumar, D. Singh, Dietary flavonoids interaction with CREB-BDNF pathway: an unconventional approach for comprehensive management of epilepsy, Curr. Neuropharmacol. 17 (2019) 1158–1175.

[10] E. Akyuz, Y.N. Paudel, A.K. Polat, H.E. Dundar, E. Angelopoulou, Enlightening the neuroprotective effect of quercetin in epilepsy: from mechanism to therapeutic opportunities, Epilepsy Behav. 115 (2021), 107701.

[11] J. Zhao, J. Yang, Y. Xie, Improvement strategies for the oral bioavailability of poorly water-soluble flavonoids: an overview, Int. J. Pharm. 570 (2019), 118642.

[12] D. Singh, Dietary flavonoids and epilepsy management, in: Treatments, Nutraceuticals, Supplements and Herbal Medicine in Neurological Disorders; Martin, Patel, and Preedy, Elsevier, 2021.

[13] C. Manach, J.L. Donovan, Pharmacokinetics and metabolism of dietary flavonoids in humans, Free Radic. Res. 38 (2004) 771–786.

[14] M. Colombo, L.R. Michels, H.F. Teixeira, L.S. Koester, Flavonoid delivery by solid dispersion: a systematic review, Phytochemistry Rev. 21 (2021) 783–808.

[15] S.S. Ferreira, A.M. Silva, F.M. Nunes, *Citrus reticulata* Blanco peels as a source of antioxidant and anti-proliferative phenolic compounds, Ind. Crop. Prod. 111 (2018) 141–148.

[16] T.S.P. Rothenbücher, J. Ledin, D. Gibbs, H. Engqvist, C. Persson, G. Hulsart-Billström, Zebrafish embryo as a replacement model for initial biocompatibility studies of biomaterials and drug delivery systems, Acta Biomater. 100 (2019) 235–243.

[17] N. Soussi-Yanicostas, Zebrafish as a model for neurological disorders, Int. J. Mol. Sci. 23 (2022) 4321.

[18] N. Rishitha, A. Muthuraman, Therapeutic evaluation of solid lipid nanoparticle of quercetin in pentylenetetrazole induced cognitive impairment of zebrafish, Life Sci. 199 (2018) 80–87.

[19] S. Kumari, A.G. Mazumder, A. Bhardwaj, D. Singh, Early α-linolenic acid exposure to embryo reduces pentylenetetrazol-induced seizures in zebrafish larva, Prostaglandins Leukot. Essent. Fatty Acids 143 (2019) 15–20.

[20] P. Sharma, P. Dhiman, D. Singh, Dietary flavonoids-rich *Citrus reticulata* peel extract interacts with CREB signaling to suppress seizures and linked neurobehavioral impairments in a kindling mouse model, Nutr. Neurosci. (2022), https://doi.org/10.1080/1028415X.2022.2071807.

[21] P. Sharma, S. Kumari, J. Sharma, R. Purohit, D. Singh, Hesperidin interacts with CREB-BDNF signaling pathway to suppress pentylenetetrazole-induced convulsions in zebrafish, Front. Pharmacol. 11 (2021), 607797.

[22] V. Dadwal, R. Joshi, M. Gupta, A multidimensional UHPLC-DAD-QTOF-IMS gradient approach for qualitative and quantitative investigation of citrus and malus fruit phenolic extracts and edibles, ACS Food Sci. Technol. 10 (2021) 2006–2018.

[23] P. Liu, J.Y. Zhou, J.H. Chang, X.G. Liu, H.F. Xue, R.X. Wang, Z.S. Li, C.S. Li, J. Wang, C.Z. Liu, Soluplus-mediated diosgenin amorphous solid dispersion with high solubility and high stability: development, characterization and oral bioavailability, Drug Des. Dev. Ther. 14 (2020) 2959.

[24] Z.M.M. Lavra, D. Pereira de Santana, M.I. Ré, Solubility and dissolution performances of spray-dried solid dispersion of Efavirenz in Soluplus, Drug Dev. Ind. Pharm. 43 (2017) 42–54.

[25] B. Tian, X. Ju, D. Yang, Y. Kong, X. Tang, Effect of the third component on the aging and crystallization of cinnarizine-soluplus® binary solid dispersion, Int. J. Pharm. 580 (2020), 119240.

[26] A.G. Mazumder, S. Kumari, D. Singh, Anticonvulsant action of a selective phosphatidylinositol-3-kinase inhibitor LY294002 in pentylenetetrazole-mediated convulsions in zebrafish, Epilepsy Res. 157 (2019), 106207.

[27] S.C. Baraban, M.R. Taylor, P.A. Castro, H. Baier, Pentylenetetrazole induced changes in zebrafish behavior, neural activity and c-fos expression, Neuroscience 131 (2005) 759–768.

[28] G. Tanwar, A.G. Mazumder, V. Bhardwaj, S. Kumari, R. Bharti, D. Singh, P. Das, R. Purohit, Target identification, screening and *in vivo* evaluation of pyrrolone-fused benzosuberene compounds against human epilepsy using Zebrafish model of pentylenetetrazol-induced seizures, Sci. Rep. 9 (2019) 1–12.

[29] R. Rajakumari, T. Volova, O.S. Oluwafemi, S. Rajesh Kumar, S. Thomas, N. Kalarikkal, Grape seed extract-soluplus dispersion and its antioxidant activity, Drug Dev. Ind. Pharm. 46 (2020) 1219–1229.

[30] X. Lian, J. Dong, J. Zhang, Y. Teng, Q. Lin, Y. Fu, T. Gong, Soluplus® based 9-nitrocamptothecin solid dispersion for peroral administration: preparation, characterization, *in vitro* and *in vivo* evaluation, Int. J. Pharm. 477 (2014) 399–407.

[31] J. Guan, L. Jin, Q. Liu, H. Xu, H. Wu, X. Zhang, S. Mao, Exploration of supersaturable lacidipine ternary amorphous solid dispersion for enhanced dissolution and *in vivo* absorption, Eur. J. Pharmaceut. Sci. 139 (2019), 105043.

[32] R.N. Shamma, M. Basha, Soluplus®: a novel polymeric solubilizer for optimization of carvedilol solid dispersions: formulation design and effect of method of preparation, Powder Technol. 237 (2013) 406–414.

[33] A.T. Serajuddin, Solid dispersion of poorly water-soluble drugs: early promises, subsequent problems, and recent breakthroughs, J. Pharmacol. Sci. 88 (1999) 1058–1066.

[34] G. Paudwal, N. Rawat, R. Gupta, A. Baldi, G. Singh, P.N. Gupta, Recent advances in solid dispersion technology for efficient delivery of poorly water-soluble drugs, Curr. Pharmaceut. Des. 25 (2019) 1524–1535.

[35] Y. Zeng, S. Li, C. Liu, T. Gong, X. Sun, Y. Fu, Z. Zhang, Soluplus micelles for improving the oral bioavailability of scopoletin and their hypouricemic effect *in vivo*, Acta Pharmacol. Sin. 38 (2017) 424–433.

[36] S. Mukesh, P. Joshi, A.K. Bansal, M.C. Kashyap, S.K. Mandal, V. Sathe, A. T. Sangamwar, Amorphous salts solid dispersions of celecoxib: enhanced biopharmaceutical performance and physical stability, Mol. Pharm. 18 (2021) 2334–2348.

[37] M. Anticona, J. Blesa, A. Frigola, M.J. Esteve, High biological value compounds extraction from citrus waste with non-conventional methods, Foods 9 (2020) 811.

[38] S. Baghel, H. Cathcart, N.J. O'Reilly, Polymeric amorphous solid dispersions: a review of amorphization, crystallization, stabilization, solid-state characterization, and aqueous solubilization of biopharmaceutical classification system class II drugs, J. Pharmacol. Sci. 105 (2016) 2527–2544.

[39] H.E. Snyder, D. Lechuga-Ballesteros, Spray drying: theory and pharmaceutical applications, in: Pharmaceutical Dosage Forms-Tablets, CRC Press, 2008, pp. 243–276.

[40] R. Jog, R. Gokhale, D.J. Burgess, Solid state drug-polymer miscibility studies using the model drug ABT-102, Int. J. Pharm. 509 (2016) 285–295.

[41] A.G. Mazumder, P. Sharma, V. Patial, D. Singh, Crocin attenuates kindling development and associated cognitive impairments in mice via inhibiting reactive oxygen species-mediated NF-κB activation, Basic Clin. Pharmacol. Toxicol. 120 (2017) 426–433.

[42] R.E. Hernandez, L. Galitan, J. Cameron, N. Goodwin, L. Ramakrishnan, Delay of initial feeding of zebrafish larvae until 8 days postfertilization has no impact on survival or growth through the juvenile stage, Zebrafish 15 (2018) 515–518.

[43] T. Hussain, S. Paranthaman, S.M.D. Rizvi, A. Moin, D.V. Gowda, G.M. Subaiea, M. Ansari, A.S. Alanazi, Fabrication and characterization of paclitaxel and resveratrol loaded soluplus polymeric nanoparticles for improved BBB penetration for glioma management, Polymers 13 (2021) 3210.

[44] A. Fleming, H. Diekmann, P. Goldsmith, Functional characterisation of the maturation of the blood-brain barrier in larval zebrafish, PLoS One 8 (2013), e77548.

[45] K. Gawel, M. Langlois, T. Martins, W. van der Ent, E. Tiraboschi, M. Jacmin, A. D. Crawford, C.V. Esguerra, Seizing the moment: zebrafish epilepsy models, Neurosci. Biobehav. Rev. 116 (2020) 1–20.

[46] M.K. Anwer, M.M. Ahmed, A. Alshetaili, B.K. Almutairy, A. Alalaiwe, F. Fatima, M. N. Ansari, M. Iqbal, Preparation of spray dried amorphous solid dispersion of diosmin in soluplus with improved hepato-renoprotective activity: *In vitro* anti-oxidant and *in-vivo* safety studies, J. Drug Deliv. Sci. Technol. 60 (2020), 102101.

[47] D.M. Labiner, L.S. Butler, Z. Cao, D.A. Hosford, C. Shin, J.O. McNamara, Induction of c-fos mRNA by kindled seizures: complex relationship with neuronal burst firing, J. Neurosci. 13 (1993) 744–751.